

MODELING OF WET DEPOSITION IN CHEMICAL TRANSPORT SIMULATION

Toshihiro KITADA

National Institute of Technology,

Gifu College

Kamimakuwa, Motosu 441-8580, Japan

Transport/chemistry/deposition model for atmospheric trace chemical species

- An important tool:
 - (1) for understanding of the effects of various human activities, such as fuel combustion and deforestation, on human health, eco-system, and climate, and
 - (2) for planning of appropriate control of emission sources.

"Comprehensive" models such as RADDM (Chang, et al., 1987); STEM-II (Carmichael, et al., 1986); and CMAQ, WRF-Chem etc. for public use

- "Comprehensive" models include not only gas/aerosol phase chemistry but also aqueous phase chemistry in cloud/rain water in addition to the processes of advection, diffusion, wet deposition (mass transfer between aqueous and gas/aerosol phases), and dry deposition.

One of the Important Factors: Wet Deposition Modeling:

Types of Modeling of Wet Deposition

1. Simple Modeling using Scavenging Coefficient.
2. Dynamic Modeling using One Dimensional Cloud Microphysics Model (Ex. RSM – RADOM scavenging module, Berkowitz et al. 1989; PLUVIUS, Hales 1981, CMAQ, WRF-Chem, others) → Hydrometeors themselves are not transported over horizontal grid cells.
3. Dynamic Modeling using Three/Two Dimensional Cloud Microphysics Model (Ex. Hegg et al. 1986, Rutledge et al. 1986, Kitada et al. 1993, others) → Allow transport of hydrometeors over horizontal grid cells.

Target for the "Comprehensive" Model Development

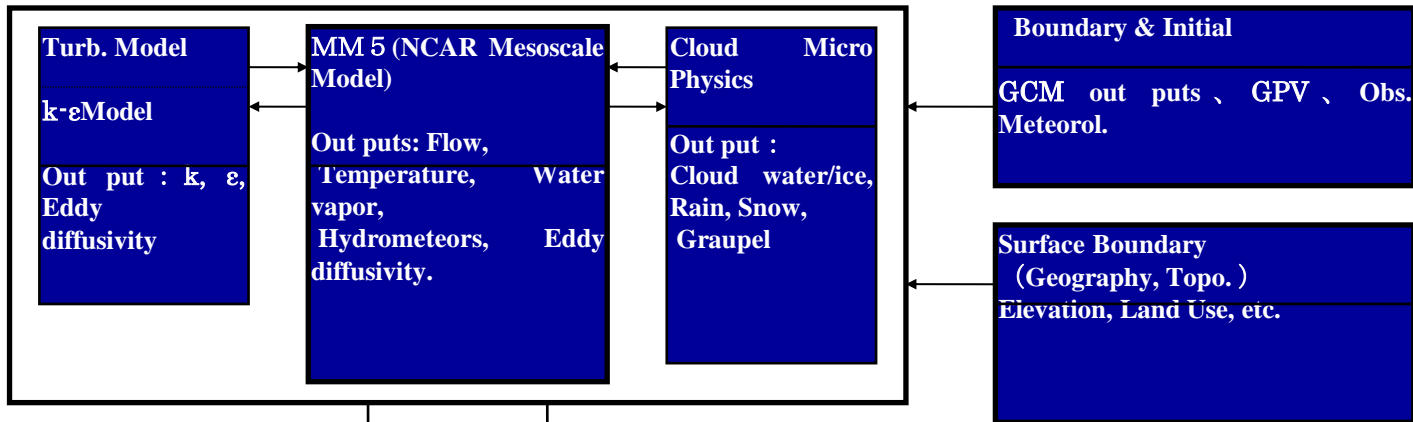
- the model which can correctly reproduce mass balance of various chemical species in the atmosphere with keeping adequate accuracy for calculated concentration distributions of chemical species.
- In the Fukushima case, radioactive species are the target.

Examples

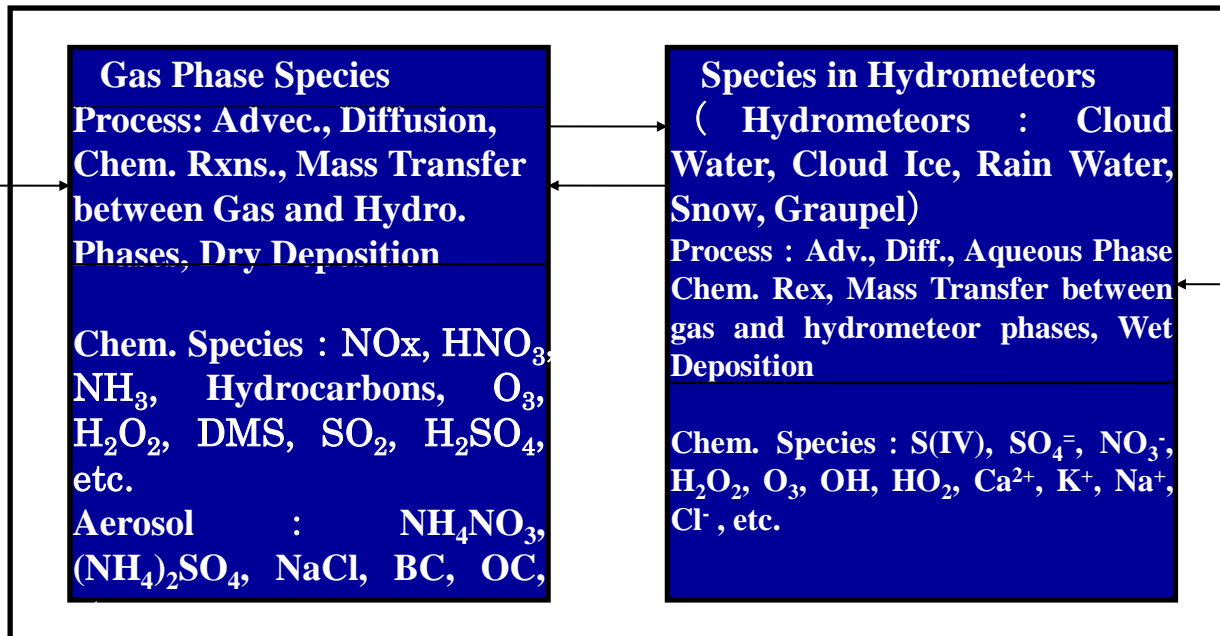
- Cloud-Resolving Modeling
- Non Cloud-Resolving Modeling: Simple Modeling of Wet Deposition

Role of Cloud in Transport/Transformation of Trace Chemical Species

METEOROLOGICAL MODEL



TRANSPORT/CHEMISTRY/DEPOSITION MODEL



Mass Conservation Eqs. of Chemical Species in hydrometeor Phases (Kitada et al., 1993)

$$\frac{\partial C_i^j q_j}{\partial t} + u \frac{\partial C_i^j q_j}{\partial x} + v \frac{\partial C_i^j q_j}{\partial y} + W_j \frac{\partial C_i^j q_j}{\partial z} - \frac{q_j \partial \rho V_j}{\rho \partial z} C_i^j = \frac{(R_i^j + {}_k T_i^j + G_i^j)}{\rho} \quad (9)$$

q_j : water content of j th hydrometeor such as cloud water, cloud ice, rain water, snow, and graupel.

C_i^j : concentration of i-th species in j-th hydrometeor.

R_i^j : chemical reaction rate of i-th species in j-th hydrometeor.

${}_k T_i^j$: mass transfer rate of i-th species between j-th and k-th hydrometeors.

G_i^j : mass transfer rate of i-th species between gas/aerosol phase and j-th hydrometeor.

Example: G^j_i for Gas Absorption/Desorption of i-th species between Gas Phase and Cloud Water and Rain Water Phases

$$G^j_i = \frac{d\rho C_i}{dt} = -4\pi a D_{g,i} \left(1 + \frac{4l}{3a\alpha}\right)^{-1} \times N \left(\rho C_i - \frac{6 \times 10^{26} C_i^j}{M_i \cdot R \cdot T \cdot H_{eff,i}} \right)$$

(molecules-*i* th species cm^{-3} -air s^{-1}) (2.25)

Mass Conservation Eqs. for Chemical Species in Gas/Aerosol Phase

$$\rho \frac{\partial C_i}{\partial t} + \rho \bar{V} \cdot \nabla C_i = \nabla \cdot \rho \tilde{K} \cdot \nabla C_i + R_i + S_i - G_i^j \quad i=1, 2, \dots, I_1 \quad (1)$$

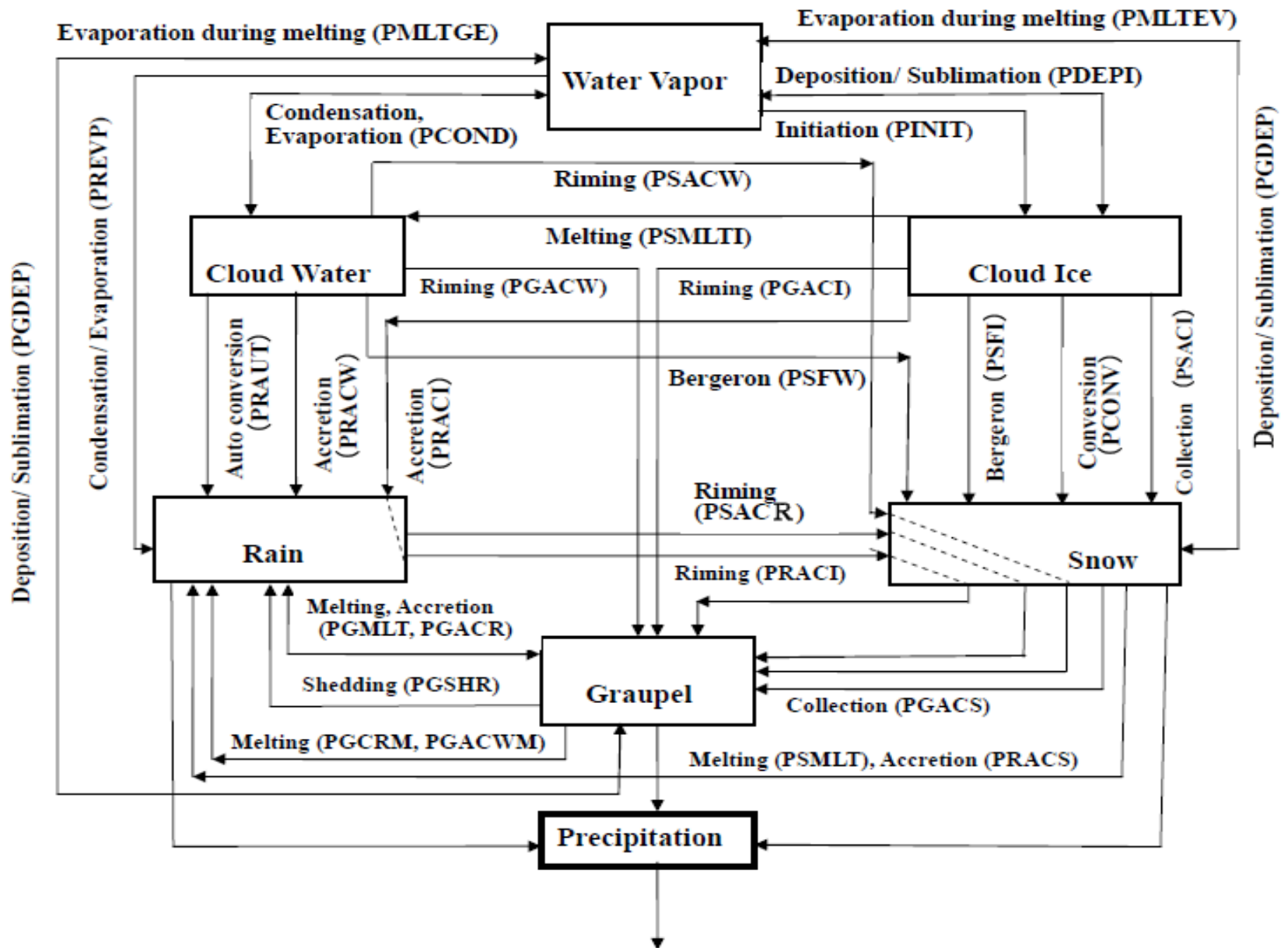


Fig. 2. Acronym diagram of inter-hydrometeor-transfers of water substance of the cloud microphysics model (after Rutledge and Hobbs, 1984).

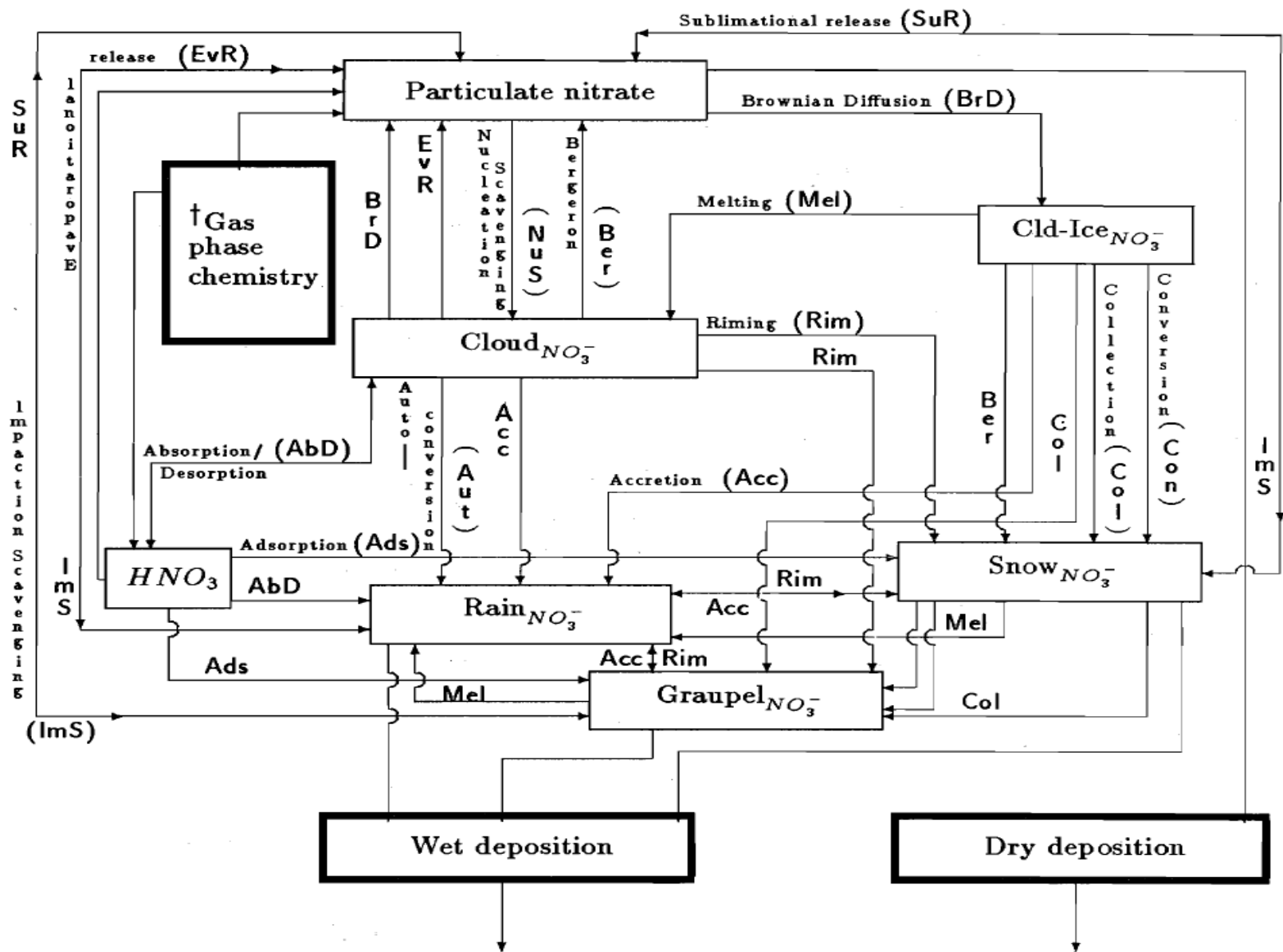
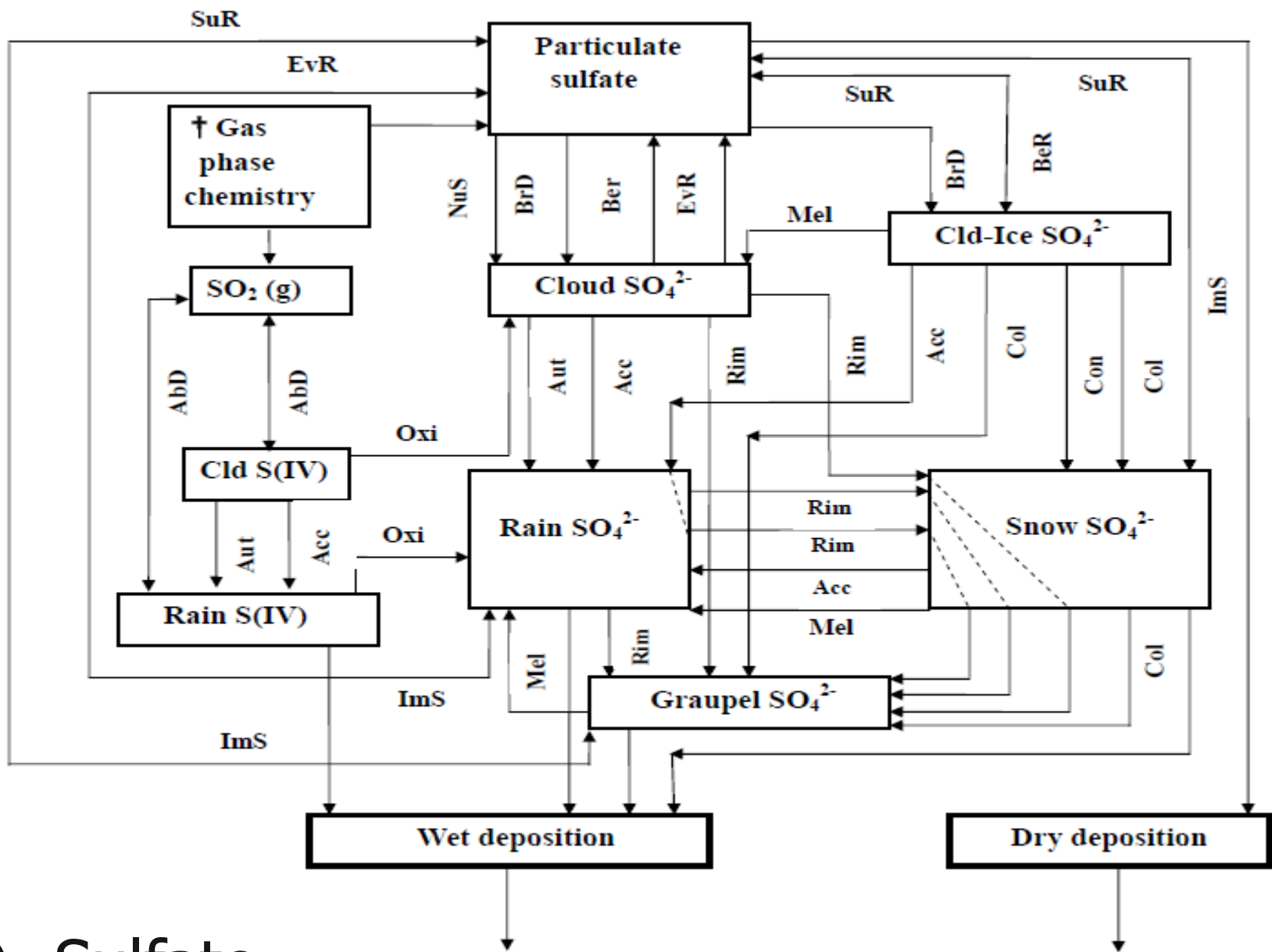


Fig. 1. Schematics showing gas-hydrometeor interphase transfers of NO_3^- adapted from Rutledge and Hobbs (1984). Normal-line boxes represent species reservoirs and thickened-line boxes represent feeding or removing processes of nitric acid and nitrate to or from these hydrometeor-phases. †The gas-phase chemistry model includes the following reactions for HNO_3 and NO_3^- productions as principal mechanisms; i.e. $\text{NO}_2 + \text{OH} \rightarrow \text{HNO}_3$, $\text{N}_2\text{O}_5 + \text{H}_2\text{O} \rightarrow 2\text{HNO}_3$, $\text{NH}_3 + \text{HNO}_3 \rightleftharpoons \text{NH}_4\text{NO}_3$.



SO_2 -Sulfate

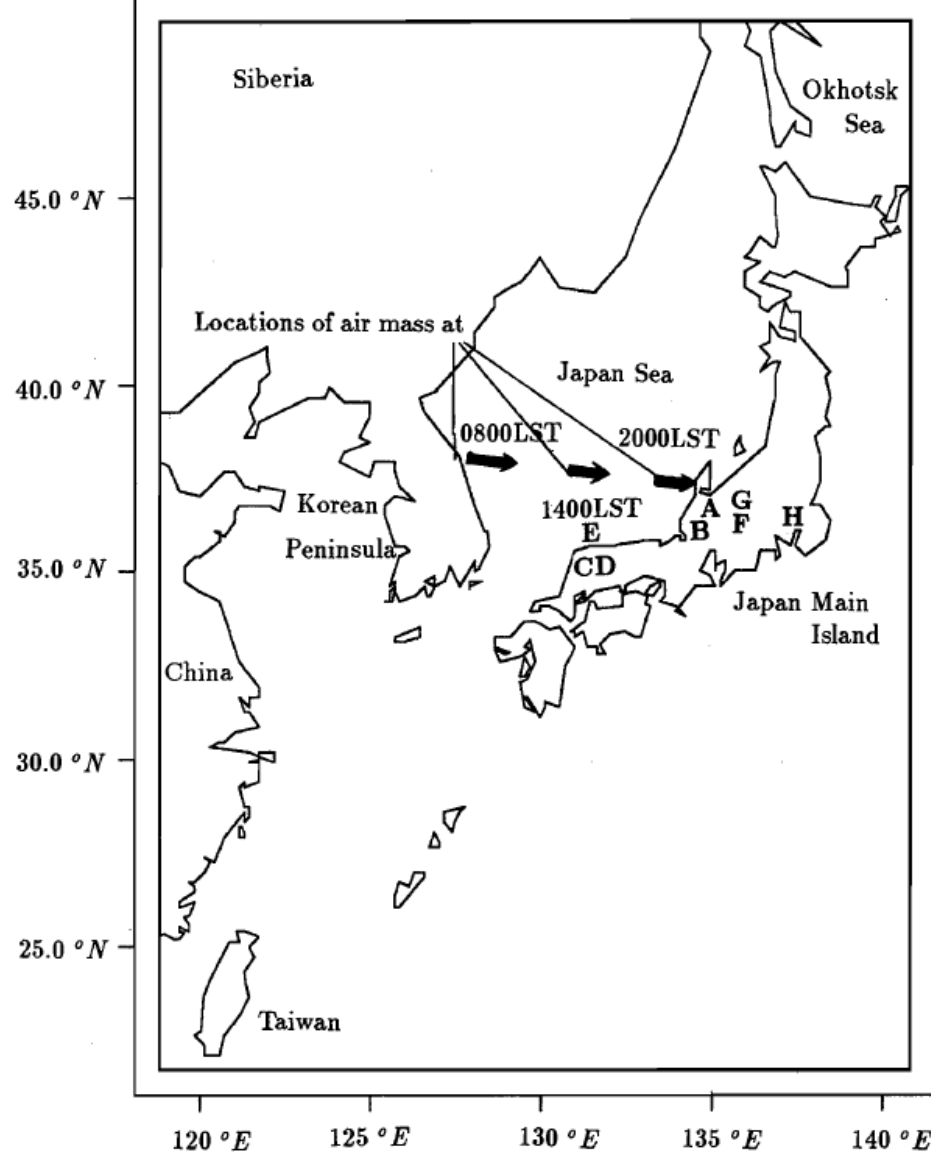


Fig. 4. The typical travelling course of the continental air mass heading over the Japan Sea in winter, which has been simulated. The locations of the air mass at 0800, 1400 and 2000 LST are indicated. The observation points of the Japanese acid snow data quoted as A-H in Section 4.4. are also marked.

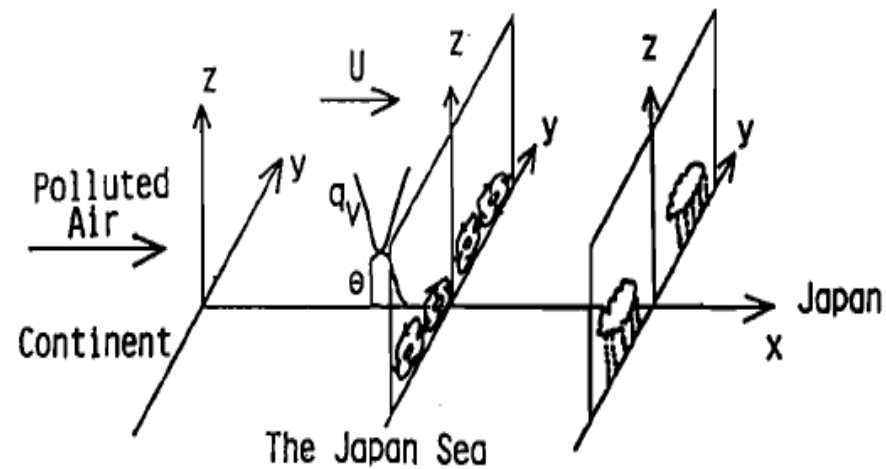


Fig. 5. Schematic diagram of the 2-D calculation domain for convective cloud streets over the Japan Sea in winter, where q_v is water vapor mixing ratio, and θ is the potential temperature.

(used in Kitada et al., 1993)

Table 3. Aqueous phase equilibrium reactions

	Reactions	Equilibrium constants M or M (atm.) ⁻¹	Source
EQ1	SO ₂ (g) ⇌ SO ₂ (aq)	1.23exp[3120·f(T)*]	PS
EQ2	SO ₂ (aq) ⇌ H ⁺ + HSO ₃ ⁻	1.23 × 10 ⁻² exp[1960·f(T)]	PS
EQ3	HSO ₃ ⁻ ⇌ H ⁺ + SO ₃ ²⁻	6.61 × 10 ⁻⁸ exp[1500·f(T)]	PS
EQ4	NH ₃ (g) ⇌ NH ₃ (aq)	75exp[3400·f(T)]	PS
EQ5	NH ₃ (aq) ⇌ NH ₄ ⁺ + OH ⁻	1.75 × 10 ⁻⁵ exp[-450·f(T)]	PS
EQ6	HNO ₃ (g) ⇌ H ⁺ + NO ₃ ⁻	2.6 × 10 ⁶ exp[8700·f(T)]	C
EQ7	CO ₂ (g) ⇌ CO ₂ (aq)	3.4 × 10 ⁻² exp[2420·f(T)]	PS
EQ8	CO ₂ (aq) ⇌ HCO ₃ ⁻ + H ⁺	4.46 × 10 ⁻⁷ exp[-1000·f(T)]	PS
EQ9	HCO ₃ ⁻ ⇌ CO ₃ ²⁻ + H ⁺	4.68 × 10 ⁻¹¹ exp[-1760·f(T)]	PS
EQ10	O ₃ (g) ⇌ O ₃ (aq)	1.13 × 10 ⁻² exp[2300·f(T)]	PS
EQ11	H ₂ O ₂ (g) ⇌ H ₂ O ₂ (aq)	7.45 × 10 ⁴ exp[6620·f(T)]	PS
EQ12	HO ₂ (g) ⇌ HO ₂ (aq)	2 × 10 ³ exp[6640·f(T)]	PS
EQ13	OH(g) ⇌ OH(aq)	25exp[5280·f(T)]	PS
EQ14	H ₂ O ⇌ H ⁺ + OH	1 × 10 ¹⁴	PS

*f(T) ≡ $\frac{1}{T} - \frac{1}{298}$ where T is temperature in K.

PS: Pandis and Seinfeld (1989).

C: Chameides (1984).

Aqueous Phase Chemical Reactions

(Kitada *et al.*, 1993).

Reactions	Rates s^{-1} , $M^{-1}s^{-1}$ or $M^{-2}s^{-1}$	Source
R1 $H_2O_2 \xrightarrow{h\nu} 2 \cdot OH$	1.0×10^{-6}	ES
R2 $OH + HO_2 \rightarrow H_2O + O_2$	$1.1 \times 10^{12} \exp[-1500/T]$	PS
R3 $OH + H_2O_2 \rightarrow H_2O + HO_2$	$8.1 \times 10^9 \exp[-1700/T]$	PS
R4 $HO_2 + HO_2 \rightarrow H_2O_2 + O_2$	$2.4 \times 10^9 \exp[-2365/T]$	PS
R5 $S(IV) + O_3 \rightarrow S(VI) + O_2$	for $SO_2(aq)$: 2.4×10^4 for HSO_3^- : $4.2 \times 10^{13} \exp[-5530/T]$ for SO_3^{2-} : $7.4 \times 10^{16} \exp[-5280/T]$	PS
R6 $S(IV) + H_2O_2 \rightarrow S(VI) + H_2O$	$3.7 \times 10^{12} \exp[-4430/T]$	PS
R7 $S(IV) + \frac{1}{2} \cdot O_2 \xrightarrow{Fe^{3+}, Mn^{2+}} S(VI)$	*	M

$$* \text{ pH} \leq 5: -4.6 \times 10^{23} \exp\left[-\frac{13,700}{T}\right] [Mn^{2+}] [HSO_3^-]$$

$$-8.8 \times 10^{15} \exp\left[-\frac{11,000}{T}\right] [Fe^{3+}] \left(\frac{[SO_2(aq)] + [HSO_3^-]}{[H^+]}\right)$$

$$\text{pH} > 5: -4.6 \times 10^{23} \exp\left[-\frac{13,700}{T}\right] [Mn^{2+}] [HSO_3^-]$$

PS: Pandis and Seinfeld (1989).

M: Martin (1984).

ES: estimated for noon time in Jan. at 40°N.

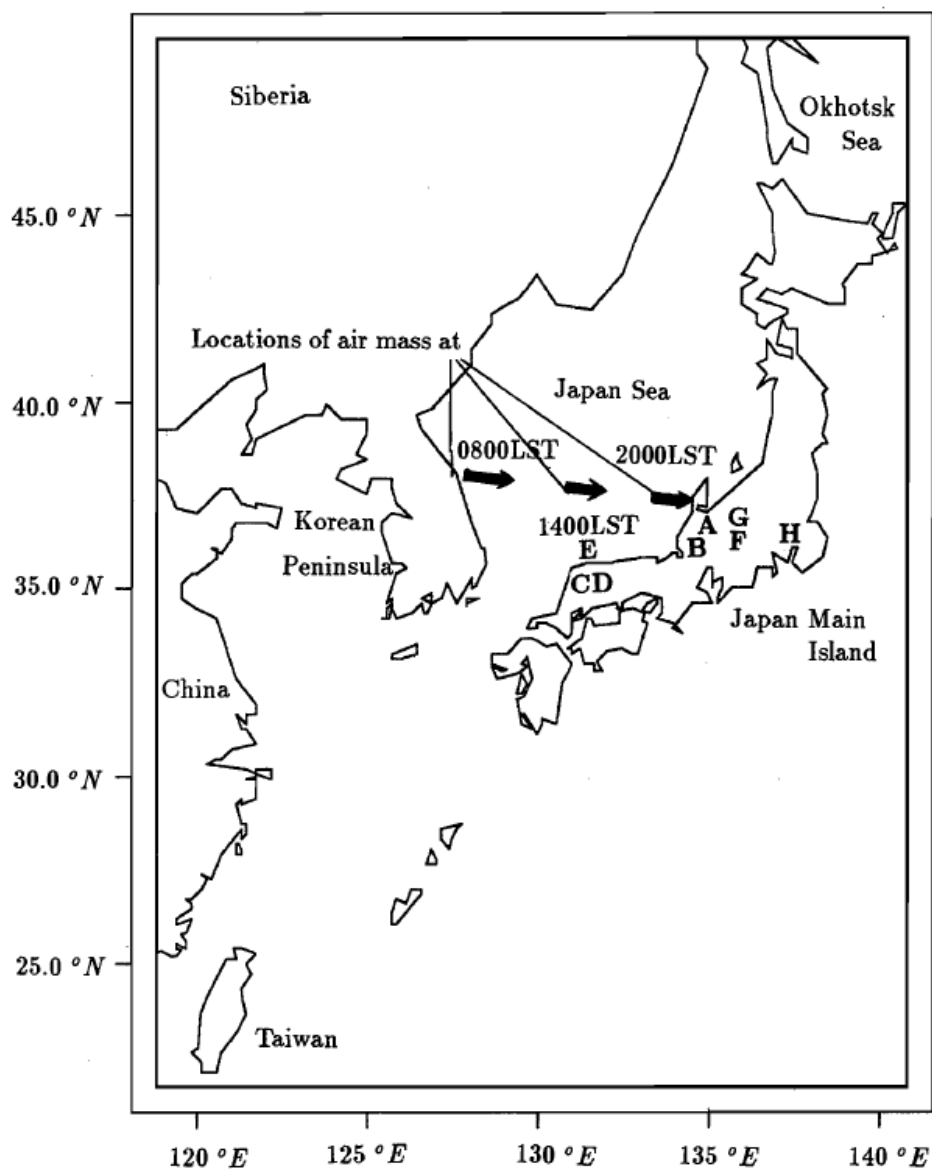


Fig. 4. The typical travelling course of the continental air mass heading over the Japan Sea in winter, which has been simulated. The locations of the air mass at 0800, 1400 and 2000 LST are indicated. The observation points of the Japanese acid snow data quoted as A-H in Section 4.4. are also marked.

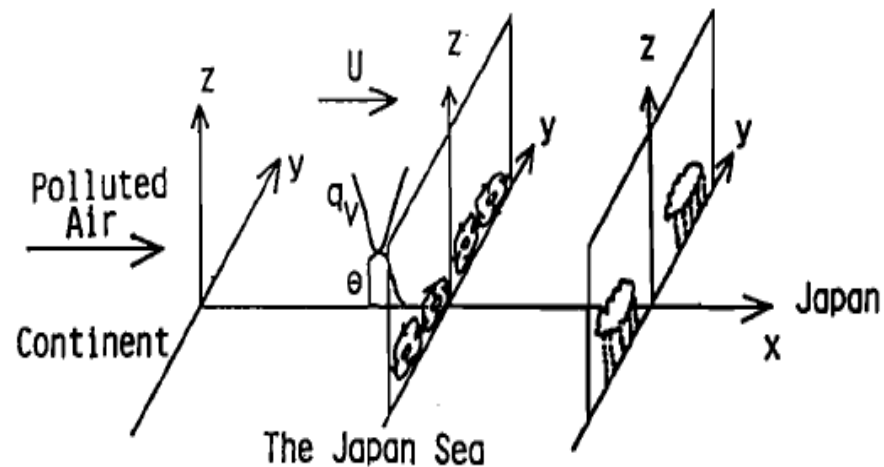


Fig. 5. Schematic diagram of the 2-D calculation domain for convective cloud streets over the Japan Sea in winter, where q_v is water vapor mixing ratio, and θ is the potential temperature.

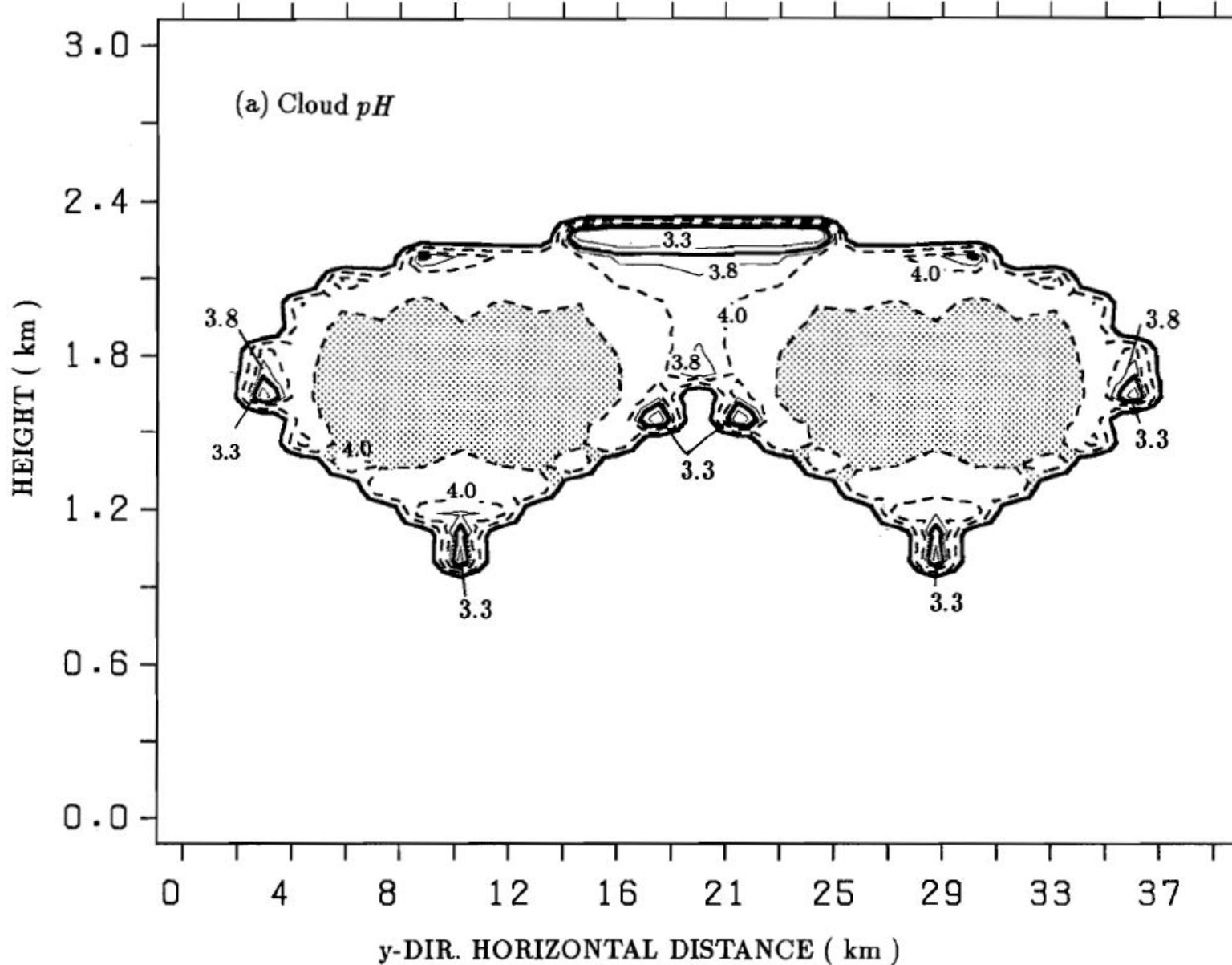


Fig. 4. Predicted contour maps of (a) cloud pH (stippling for pH > 4.4), and (b) cloud NO_3^- (stippling for concentration > 5) and (c) cloud SO_4^{2-} (stippling for concentration > 3) at 2000 LST, in nmole kg-air^{-1} .

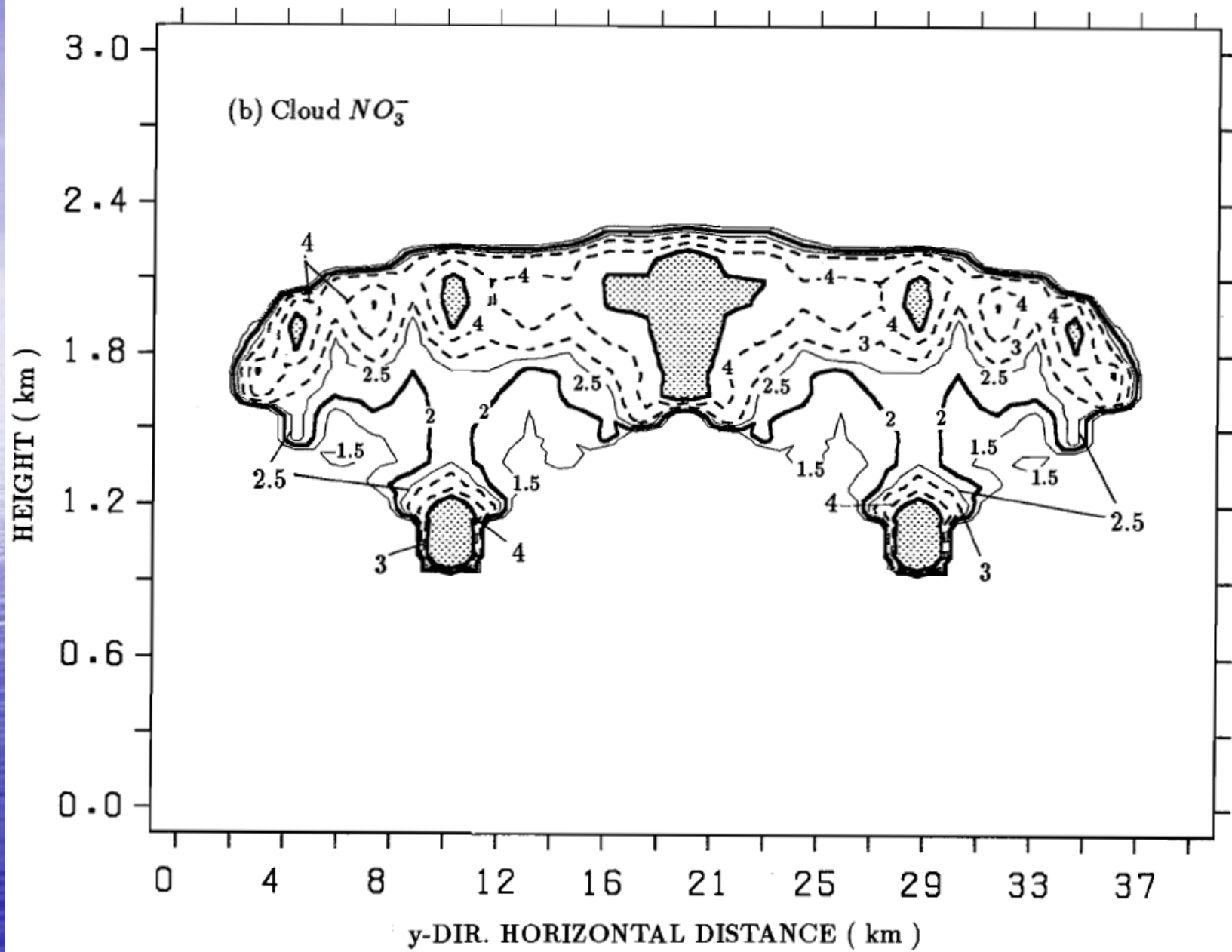


Fig. 4. (Continued)

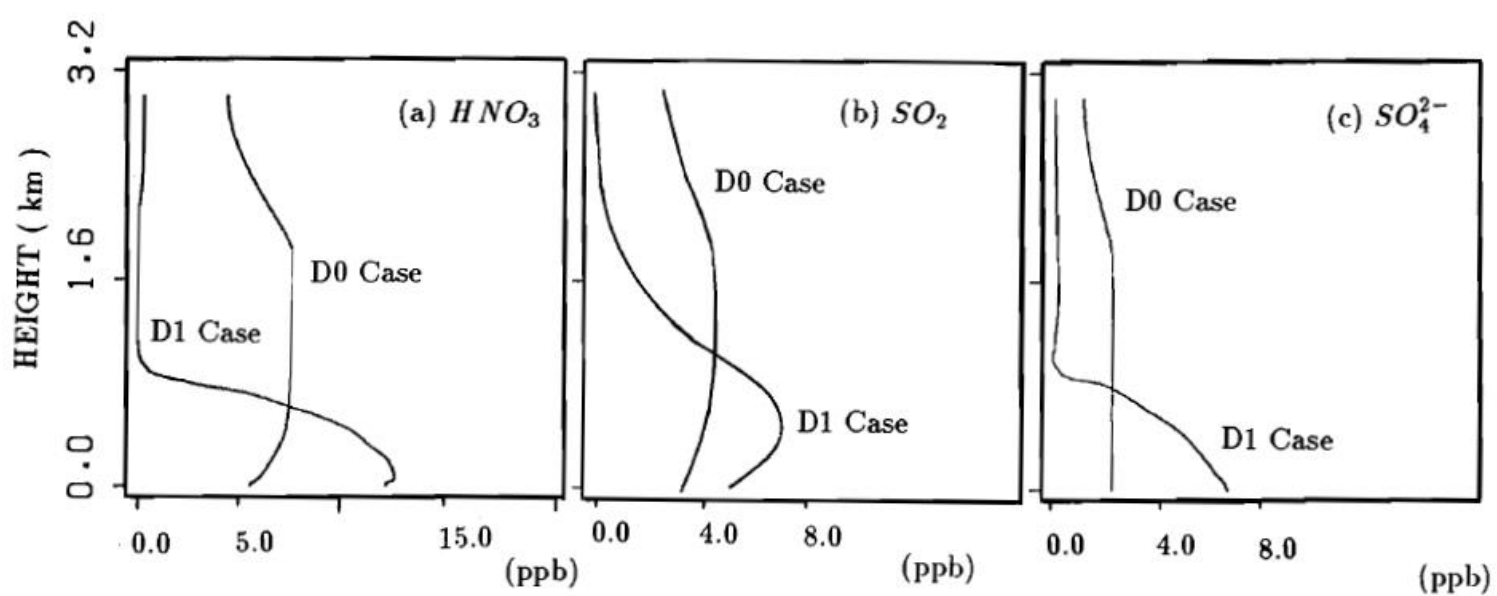


Fig. 1. Comparison of predicted vertical profiles of gas-phase concentrations (ppb), between D0 (no-cloud) and D1 (with-cloud) cases: (a) HNO_3 , (b) SO_2 and (c) SO_4^{2-} at 2000 LST along $y|_{\max, \text{updraft}} = 10.5$ km.

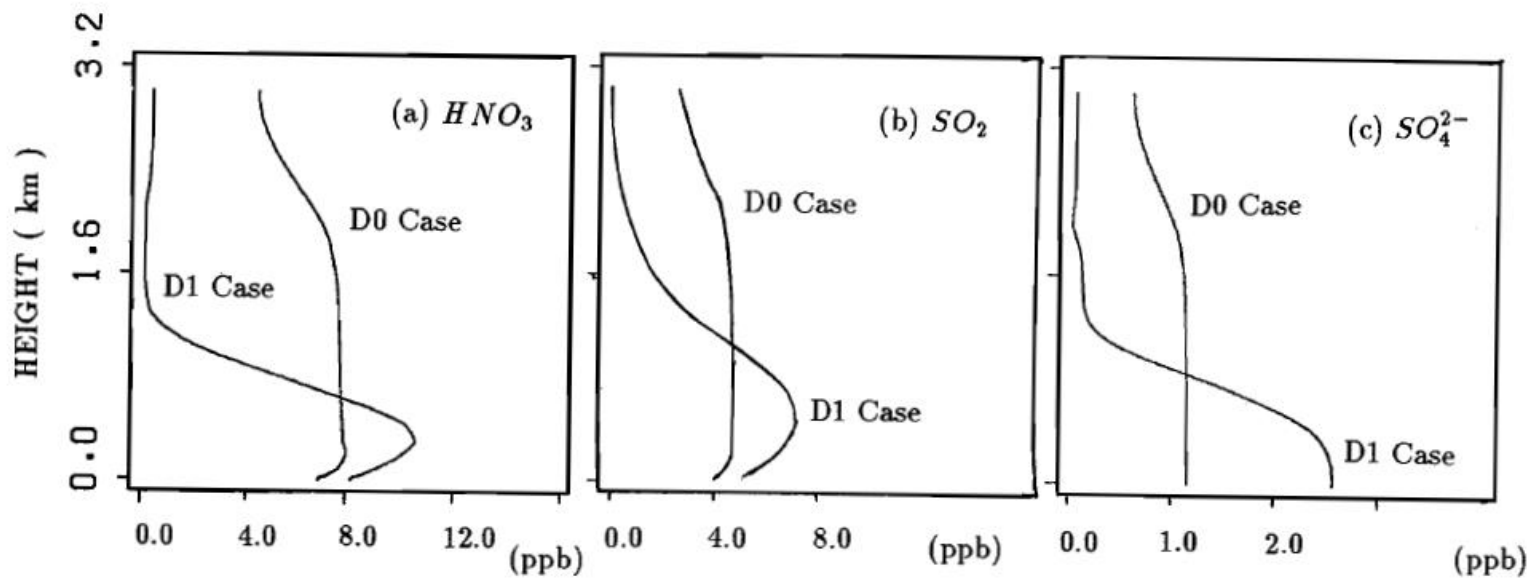


Fig. 2. Same as in Fig. 1, but for $y|_{\max, \text{downdraft}} = 19.5$ km.

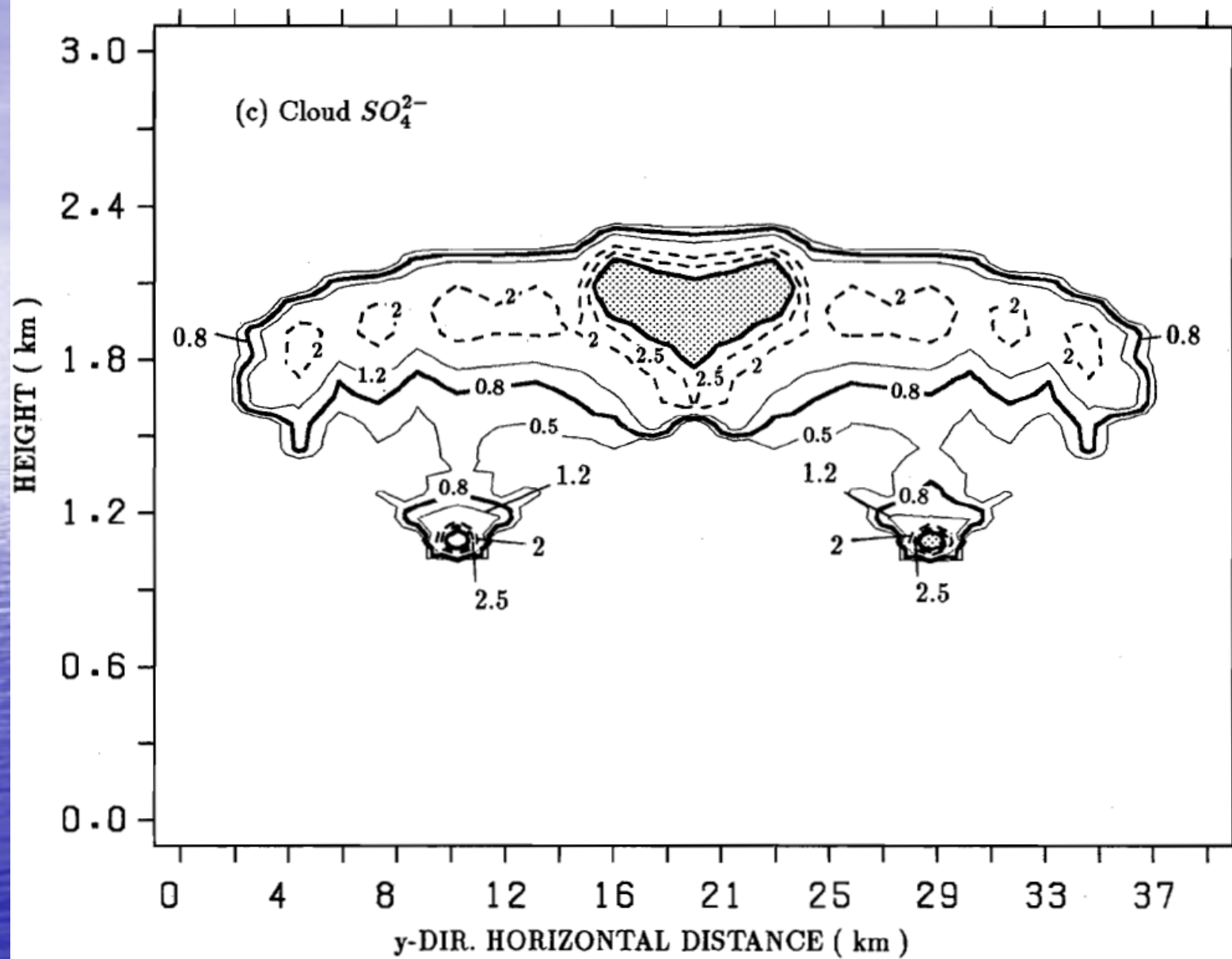


Fig. 4. (Continued)

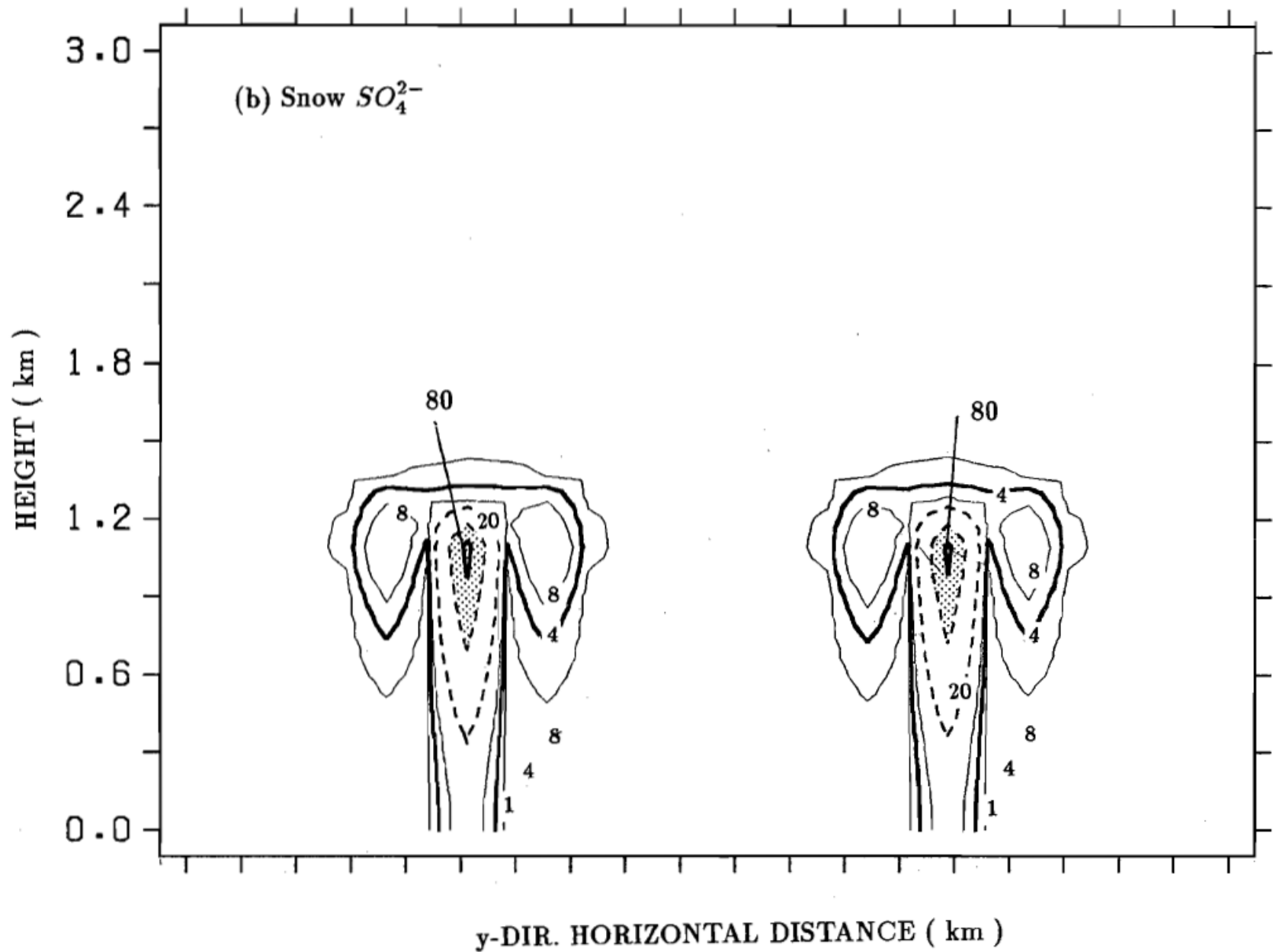


Fig. 6. (Continued)

Examples

- Cloud-Resolving Modeling
- Non Cloud-Resolving Modeling: Simple Modeling of Wet Deposition

CTM Equations System for Large Scale

$$\begin{aligned}
 C \frac{\partial X_i}{\partial t} + CU \frac{\partial X_i}{\partial x} + CV \frac{\partial X_i}{\partial y} + C\dot{\sigma} \frac{\partial X_i}{\partial \sigma} = \frac{\partial}{\partial x} \left(CE_\phi \frac{\partial X_i}{\partial x} \right) + \\
 \frac{1}{\cos \theta} \frac{\partial}{\partial y} \left(C \cos \theta E_\theta \frac{\partial X_i}{\partial y} \right) + \frac{\rho g^2}{\pi^2 r^2} \frac{\partial}{\partial \sigma} \left(C \rho r^2 E_\sigma \frac{\partial X_i}{\partial \sigma} \right) + R_i - \underline{\Lambda C X_i}, \quad i = 1, 2, \dots, I
 \end{aligned}
 \tag{3}$$

where $dx = r \cos \theta d\phi$, $dy = r d\theta$, $\sigma = (P - P_T)/\pi$, $\pi = P_S - P_T$, $\dot{\sigma} = \left\{ \left(\frac{\partial z}{\partial t} \right)_\sigma + \vec{V} \cdot \nabla_\sigma z - W \right\} \frac{\rho g}{\pi}$. X_i is the non-dimensional concentration of the i^{th} chemical species; ρ the air density in kg m^{-3} ; C the air density in kmol m^{-3} ; θ and ϕ denote latitude and longitude, respectively; r is the distance from the center of the Earth (approximated by the averaged radius of the earth); P_S and P_T denote the atmospheric pressures at the earth's surface and the top

Below top of cloud layer: scavenging of gas/aerosol phase species by hydrometeors,

$$\frac{\partial C X_i}{\partial t} = -\Lambda C X_i \quad (9)$$

For rain,

$$\Lambda_{p,rain} = 6 \times 10^{-4} \eta_r P^{0.75} \quad (2)$$

where $\Lambda_{p,rain}$ denotes the scavenging coefficient for particle due to rain in s^{-1} , η_r the collection efficiency of aerosol by rain and was assumed to be $0.3 \sim 0.5$, and P the precipitation intensity in $mmhr^{-1}$.

For snow, following Slinn (1974),

$$\Lambda_{p,snow} = \frac{\rho_w g \eta_s (3.6 \times 10^{-6} P)}{\rho_a V_t^2} \quad (3)$$

where ρ_w denotes the density of water ($= 1000 \text{ kgm}^{-3}$), g the gravitational acceralation ($= 9.8 \text{ ms}^{-2}$), ρ_a the air density ($\sim 1 \text{ kg m}^{-3}$), V_t the average settling velocity of the snow flakes in ms^{-1} and is expressed by the following equation recommended by Knutson *et al.* (1976):

$$V_t = (102 + 51 \log_{10} d_c) / 100 \quad (4)$$

where d_c denotes the diameter of the circle circumscribed about the average snowflake in cm. $\Lambda_{p,snow}$ in Eq.(3) was approximated as $5.6 \times 10^{-4} P$ by assuming $d_c = 500 \mu\text{m}$ and $\eta_s = 0.002$ (judged from figure in Slinn, 1977).

Coefficients (s^{-1}) for scavenging, due to rain, of gaseous species were given in the model, for example, for SO_2 ,

$$\Lambda_{SO_2} = \beta \frac{\alpha P}{3.6H} \quad (5)$$

$$\alpha = 10^{-6} R T H_{eff,SO_2} \quad (6)$$

where H denotes the height of cloud-top in m, R the universal gas constant ($= 0.082 \ell \text{ atm K}^{-1} \text{ mol}^{-1}$), T the air temperature in K, and H_{eff,SO_2} the inverse of the effective Henry's law

Simple Modeling of Wet Deposition: Ex. For Particulate Sulfate (derived and summarized in Kitada, 1994)

Formulation by Scavenging Rate Coefficient Λ :

$$\frac{d(\text{SO}_4^{2-})_r}{dt} = - \frac{d(\text{SO}_4^{2-})_g}{dt} = \Lambda (\text{SO}_4^{2-})_g \quad (2.11)$$

$(\text{SO}_4^{2-})_r$ Mass conc. of "sulfate in rain phase".

$(\text{SO}_4^{2-})_g$ Mass conc. of "sulfate in gas/aerosol phase".

Λ : Capture rate of sulfate by rain with collection efficiency " η " of sulfate particle (radius R) by rain drop (radius, a)

$$\Lambda = \pi \int_0^{\infty} a^2 V(a) \eta(a, R) N(a) da \quad (2.12)$$

Simple Modeling of Wet Deposition: Ex. For Particulate Sulfate (derived and summarized in Kitada, 1994) (continued)

Simplified Expression of Λ using volume averaged radius of rain drop " a_m " (Slinn, 1977) :

$$\Lambda \cong \frac{\eta(a_m, R)}{a_m} \int_0^{\infty} \pi V(a) N(a) a^3 da \quad (2.13)$$

Precipitation intensity P :

$$P = \int_0^{\infty} V(a) N(a) \frac{4\pi}{3} a^3 da \quad (2.14)$$

Simplified form of Λ ($C=3/4$, constant):

$$\Lambda = C \frac{P \eta(a_m, R)}{a_m} \quad (2.15)$$

(continued)

Empirical relation of a_m and P (Mason, 1971):

$$a_m \cong 0.35 P^{0.25} \quad (2.16)$$

$$\Lambda = \frac{C}{0.35} \eta P^{0.75} \quad (\text{h}^{-1}) = 6 \times 10^{-4} \eta P^{0.75} \quad (\text{s}^{-1})$$

$(C \equiv \frac{3}{4}, \text{constant})$

If we choose, for example, $\eta = 0.05$,

$$\Lambda = 3 \times 10^{-5} P^{0.75} \quad (\text{s}^{-1})$$

From semi-empirical expression by Slinn (1977), sample value of η for particle with its radius $0.1 \sim 3 \mu\text{m} \rightarrow$

半径 0.1mm の雨粒子の場合

$$\eta = 8 \times 10^{-4} \sim 10^{-1}$$

半径 1mm の雨粒子の場合

$$\eta = 2 \times 10^{-4} \sim 3 \times 10^{-1}$$

代表長 $10 \mu\text{m}$ の雪粒子の場合

$$\eta = 2 \times 10^{-4} \sim 0.1$$

代表長 $50 \mu\text{m}$ の雪粒子の場合

$$\eta = 2 \times 10^{-4} \sim 7 \times 10^{-3}$$

代表長 $1000 \mu\text{m}$ の雪粒子の場合

$$\eta = 10^{-4} \sim 5 \times 10^{-4}$$

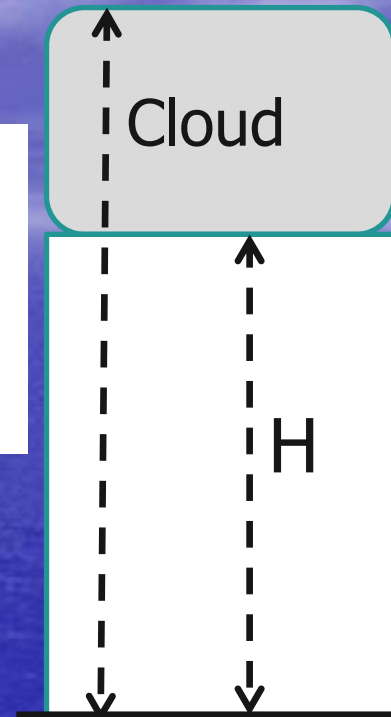
(continued)

By a variable transformation of $dt = -dz/V(a_m)$ Eq. 2.11 can be written as follows:

$$V(a_m) \frac{d(\text{SO}_4^{2-})_r}{dz} = -\Lambda(\text{SO}_4^{2-})_g$$

Integrating from $z=0 \sim H$:

$$V(a_m) \left\{ (\text{SO}_4^{2-})_r^0 - (\text{SO}_4^{2-})_r^H \right\} = \int_0^H \Lambda(\text{SO}_4^{2-})_g dz \quad (2.19)$$



Wet Deposition at Ground Level,
 F_w , can be obtained by evaluating
the right hand side of Eq. (2.20):

$$F_w \equiv V(a_m) (\text{SO}_4^{2-})_r^0 = \int_0^H \Lambda (\text{SO}_4^{2-})_g dz + V(a_m) (\text{SO}_4^{2-})_r^H \quad (2.20)$$

$(\text{SO}_4^{2-})_r^0$: Sulfate mass in rain water phase at ground level.

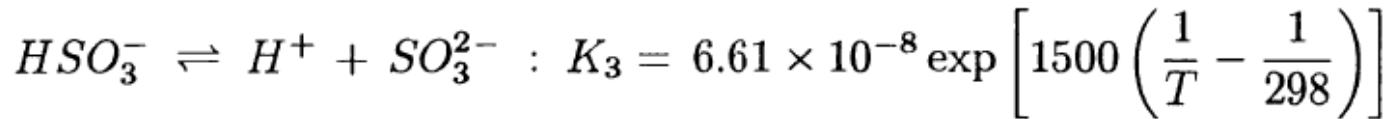
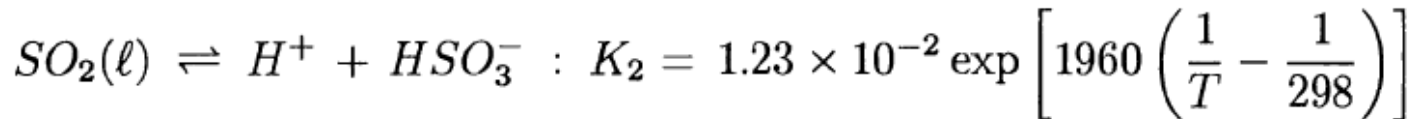
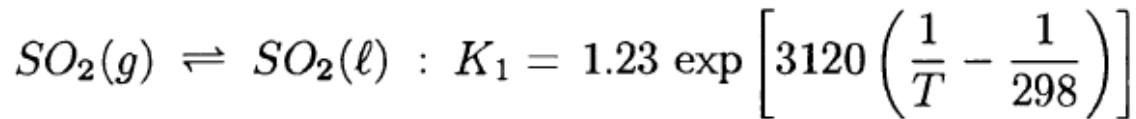
$(\text{SO}_4^{2-})_r^H$: Sulfate in rain at height of cloud base H; $(\text{SO}_4^{2-})_r^H$ may not be zero at $z = H$.

In gas absorption/desorption case, conc. in rain water must be considered in wet dep.:

constant for SO_2 in mole $\ell^{-1} \text{ atm}^{-1}$, which is a function of the hydrogen ion concentration in rain drop, and is defined as:

$$H_{eff,SO_2} = K_1 \left(1 + \frac{K_2}{[H^+]} + \frac{K_2 K_3}{[H^+]^2} \right) \quad (7)$$

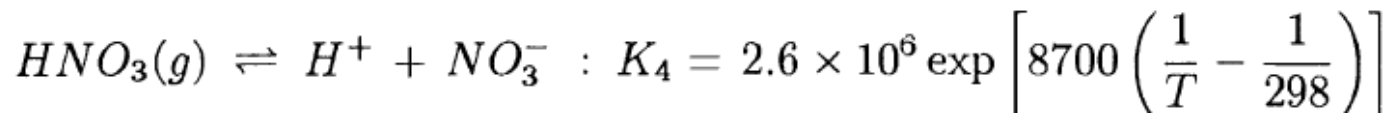
where K_1 , K_2 , and K_3 are equilibrium constants of the following reactions with concentrations in atm and M:



For absorption of HNO_3 ,

$$H_{eff,HNO_3} = \frac{K_4}{[H^+]} \quad (8)$$

where K_4 denotes equilibrium constant for



(continued)

For example, the estimated value of α is 0.671 for pH = 5.6 at 273 K, 0.330 for pH = 5.3 at 273 K and 0.089 for pH = 5.0 at 298 K. Equation (5) has been derived by assuming that S(IV) concentration in precipitation can be expressed with the hypothetical concentration of S(IV) which is in equilibrium with the atmospheric SO₂ concentration averaged over the height from ground to cloud-top. The factor β in Eq.(5) is an “equilibrium index” and represents the ratio of the real S(IV)- to the hypothetical equilibrium S(IV)-concentrations in precipitation, and was assumed unity for the SO₂,-S(IV) system. Expression similar to Eq. (5) was used also for HNO₃ and H₂O₂, where the “equilibrium” ratio β was given as 0.38×10^{-8} for HNO₃ and 0.055 for H₂O₂; these values were determined by a series of numerical experiments in which temporal development of various chemical species in a water drop, falling through pollutants-containing-atmosphere, was calculated using a sub-module of a comprehensive acid rain mode

Calculated S and N Deposition for March 1 to 15, 1994

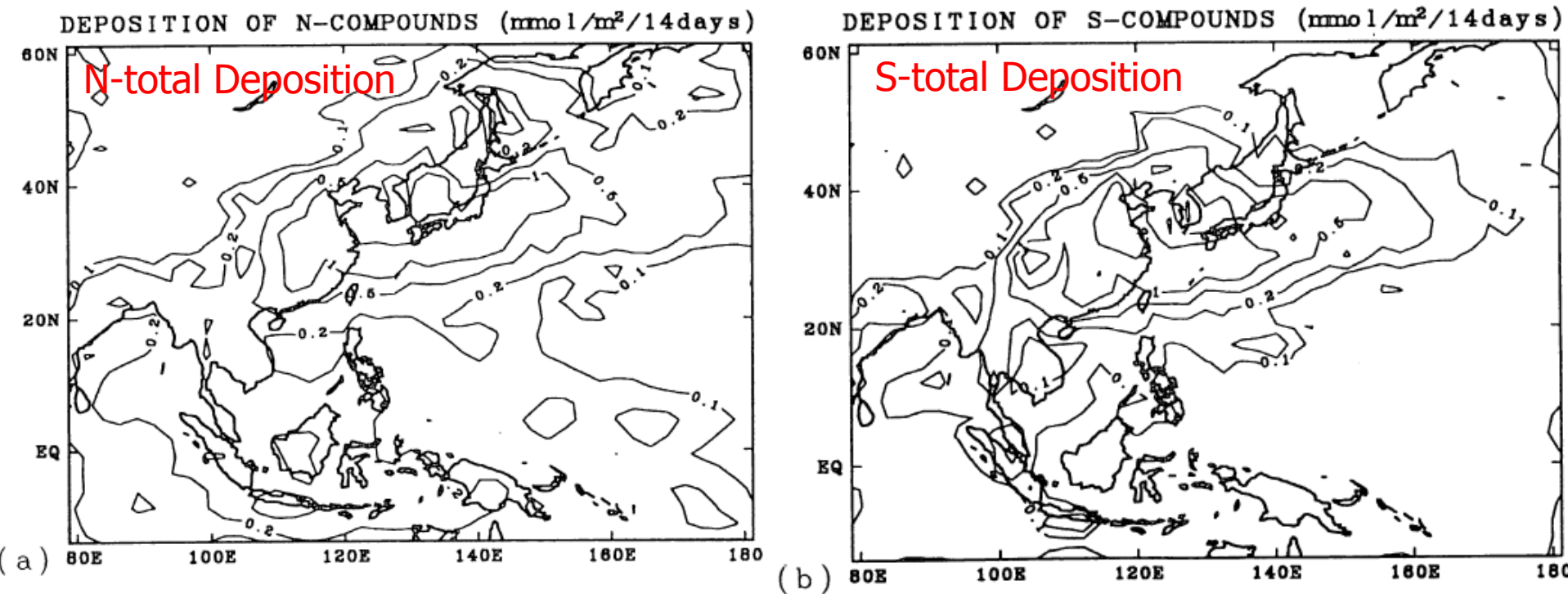


Figure 5. Calculated dry + wet deposition (BASE) of (a) N- and (b) S-compounds in $\text{mmol m}^{-2} (14\text{day})^{-1}$. The fourteen day stands for the period from 00GMT, 1 March to 00GMT, 15 March, 1994. Contour lines : 0.1, 0.2, 0.5, 1, and 2.

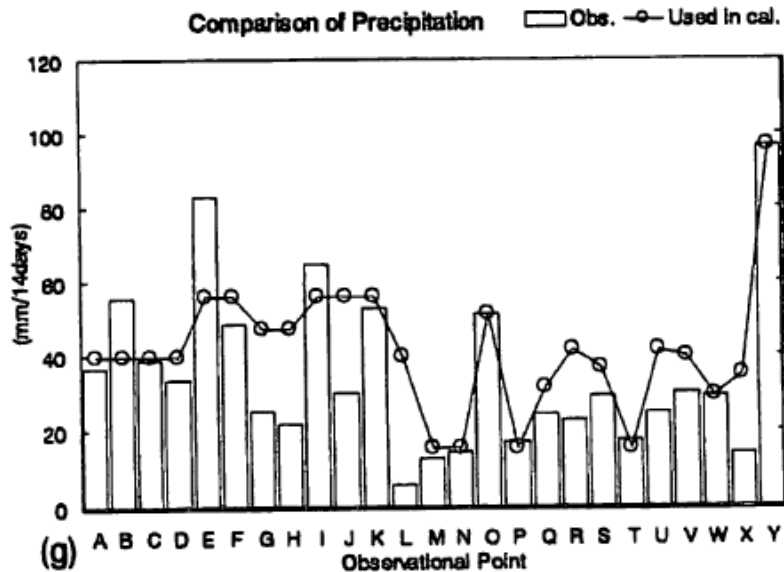


Figure 8. (Continued)

OBSERVATIONAL POINTS

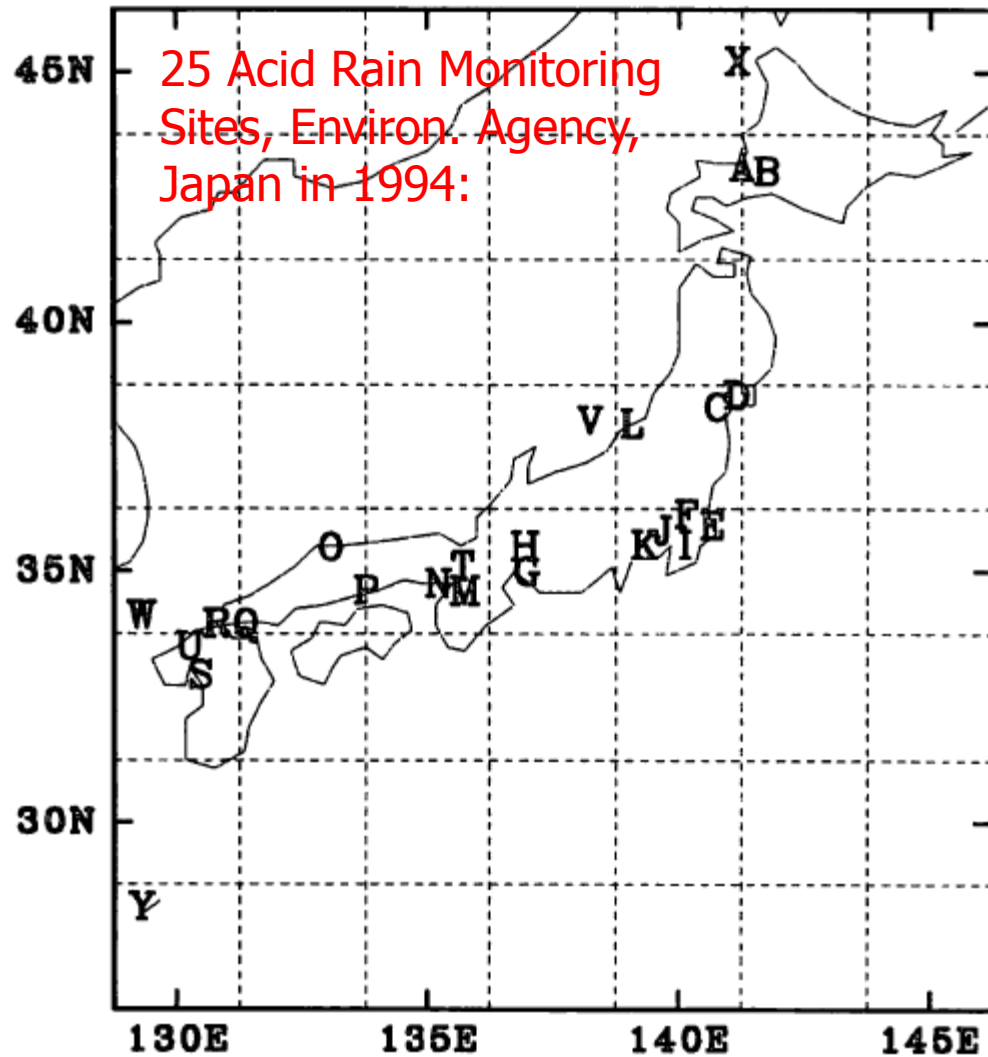


Figure 9. Observation points for acid deposition : points A through Y. One grid cell written with dashed lines expresses area of $2.5^{\circ} \times 2.5^{\circ}$. See also caption for Fig. 8.

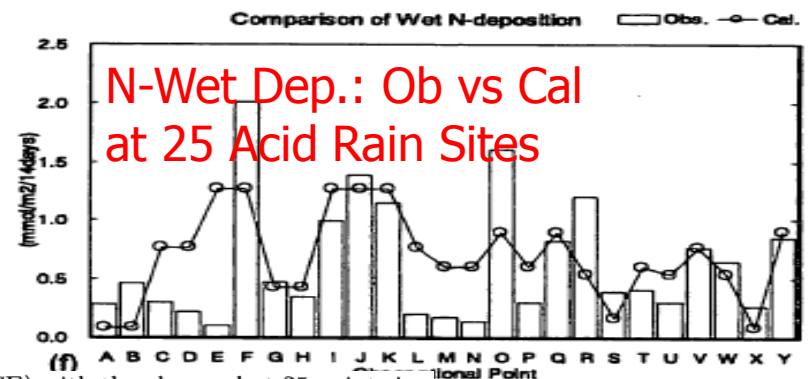
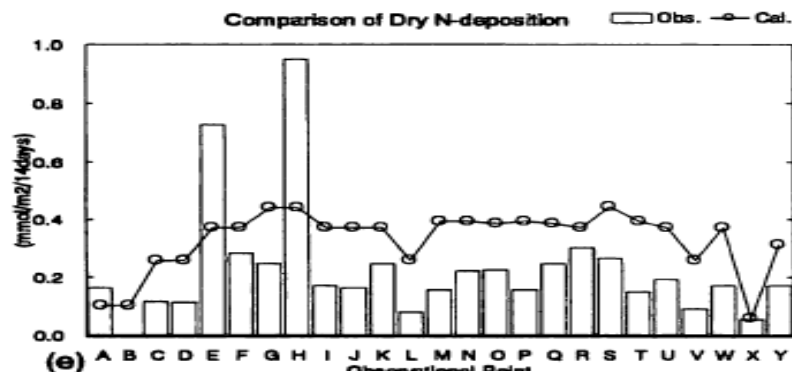
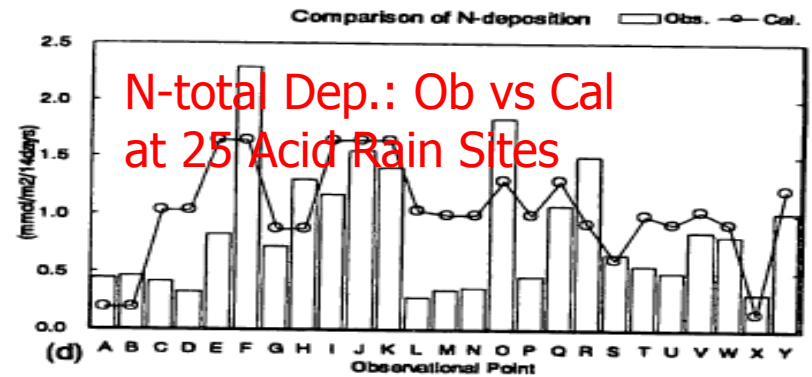
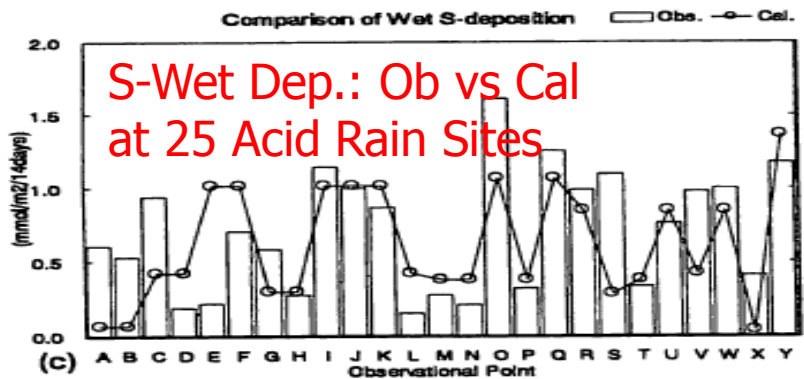
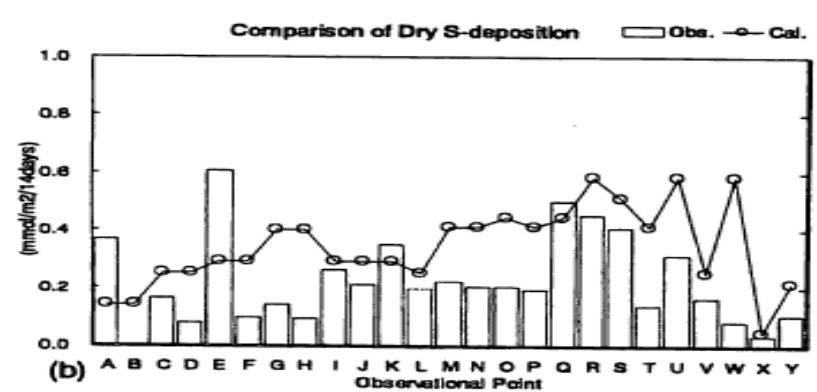
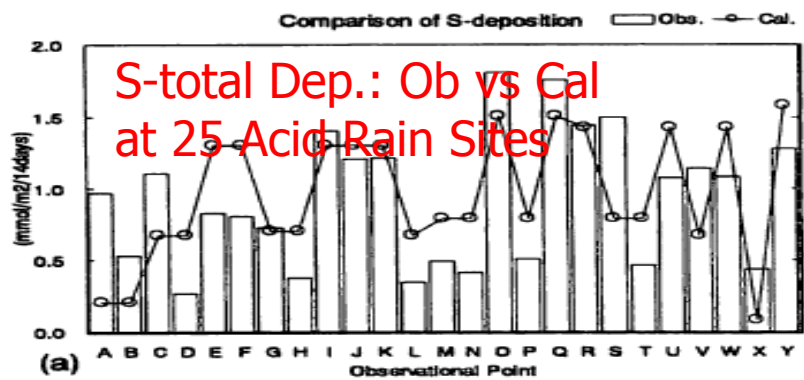
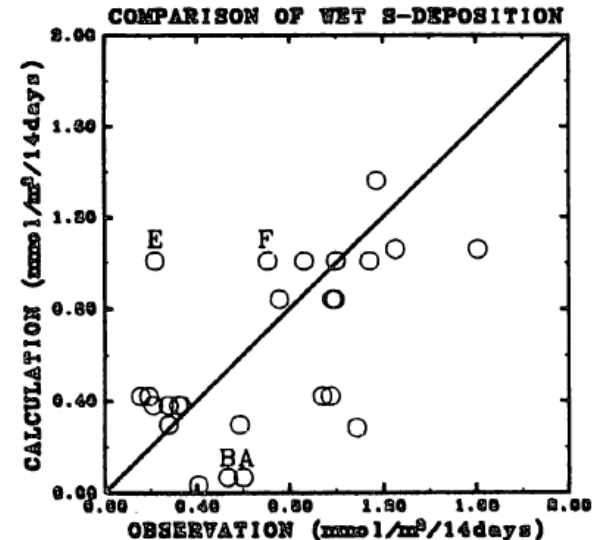
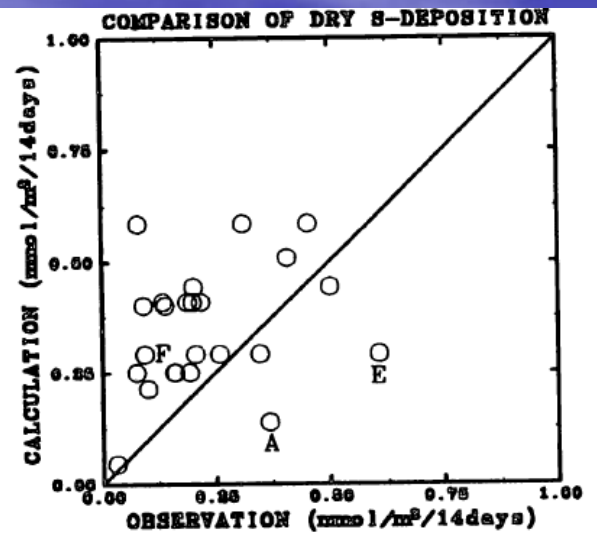
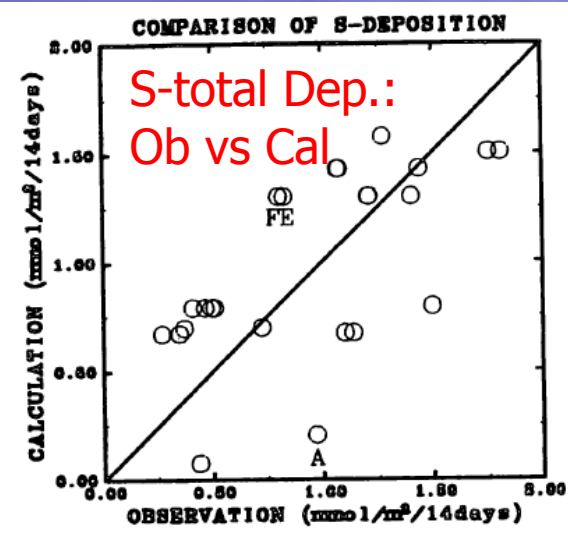


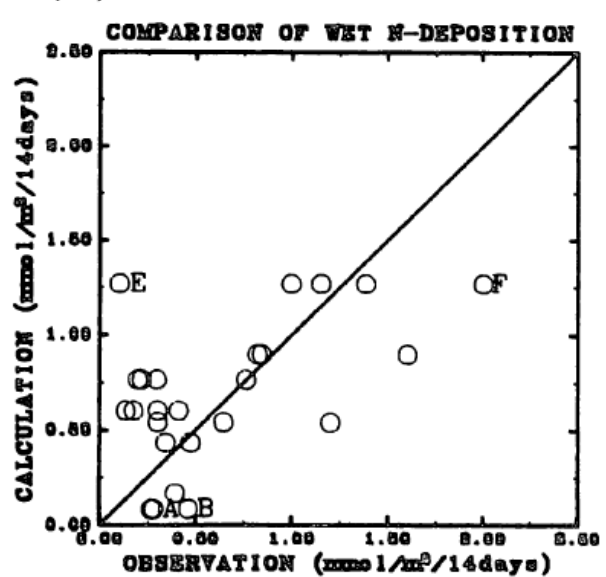
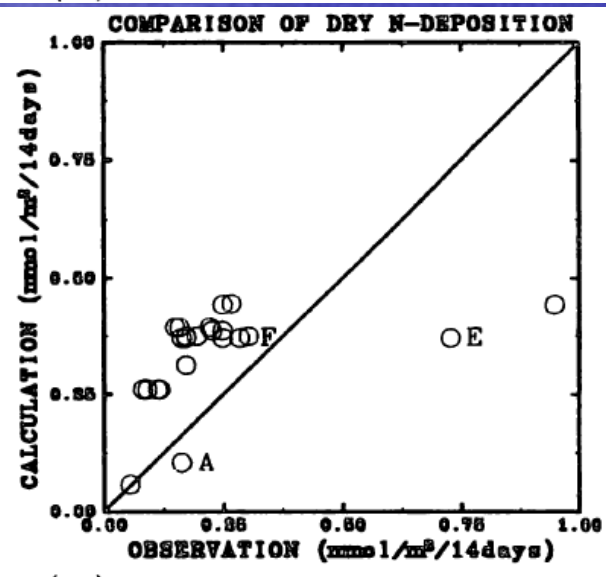
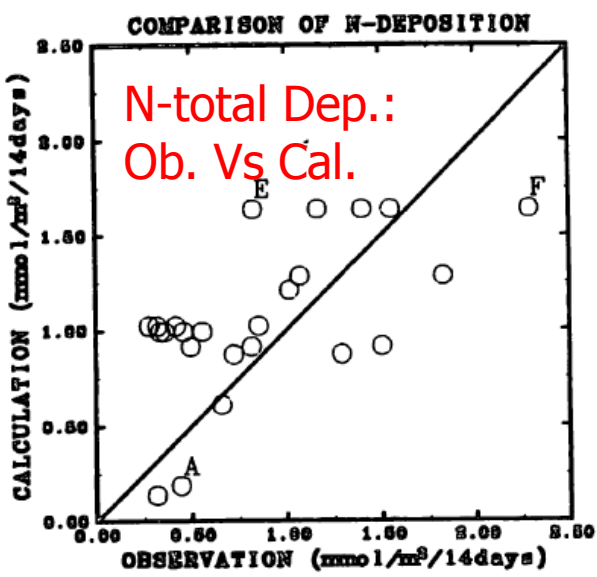
Figure 8. Comparison of the calculated deposition (BASE) with the observed at 25 points in Japan : (a) S-total-, (b) S-dry-, and (c) S-wet-depositions, where S-compounds denote SO_2 and SO_4^{2-} ; (d) N-total-, (e) N-dry-, (f) N-wet-depositions, where N-compound means HNO_3 (NO_3^-) : Fig. 8(g) shows precipitation : the observation with bar graph and the data (Xie and Arkin, 1995) used in the present simulation. Observation points : A-Sapporo, B-Nohoro, C-Sendai, D-Eno-dake, E-Kashima, F-Tsukuba, G-Nagoya, H-Inuyama, I-Ichihara, J-Tokyo, K-Kawasaki, L-Niigata, M-Osaka, N-Amagasaki, O-Matsue, P-Kurashiki, Q-Ube, R-Kitakyusyu, S-Omuta, T-Kyoto-Hachiman, U-Chikugo-Ogori, V-Sado, W-Tsushima, X-Rishiri, and Y-Amami. The locations of these points are shown in Fig. 9.



(a) ○:BASE

(b) ○:BASE

(c) ○:BASE



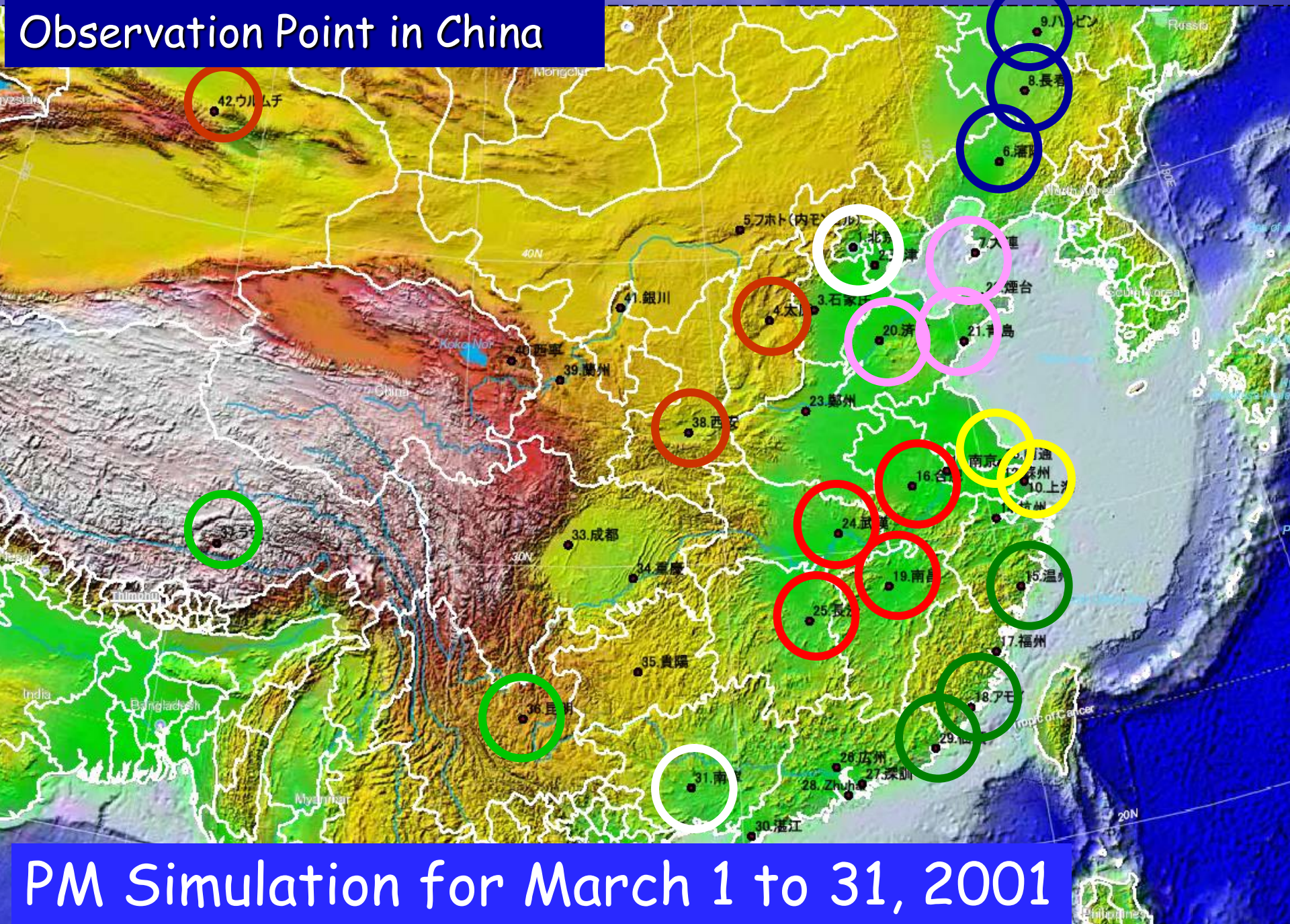
(d) ○:BASE

(e) ○:BASE

(f) ○:BASE

Figure 10. Calculated(BASE in Table 2) VS. observed depositions at the points A through Y in Fig. 9 : (a) S-total-, (b) S-dry-, and (c) S-wet-depositions ; similarly (d) N-total-, (e) N-dry-, and (f) N-wet-depositions. The N-wet-deposition includes that of HNO_3 (NO_3^-). The letter A indicates Sapporo, B Nohoro, E Kashima and F Tsukuba. At Nohoro (i.e. B), only wet-deposition was observed.

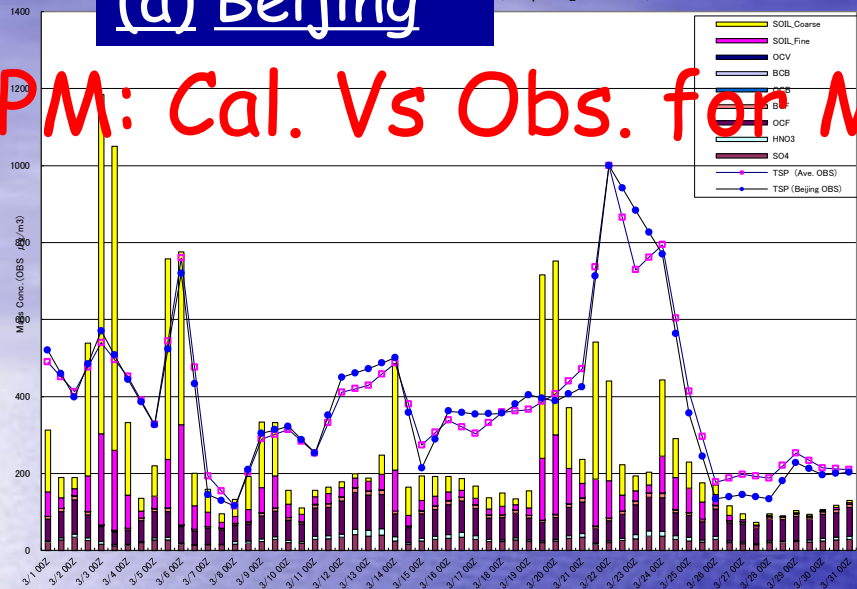
Observation Point in China



PM Simulation for March 1 to 31, 2001

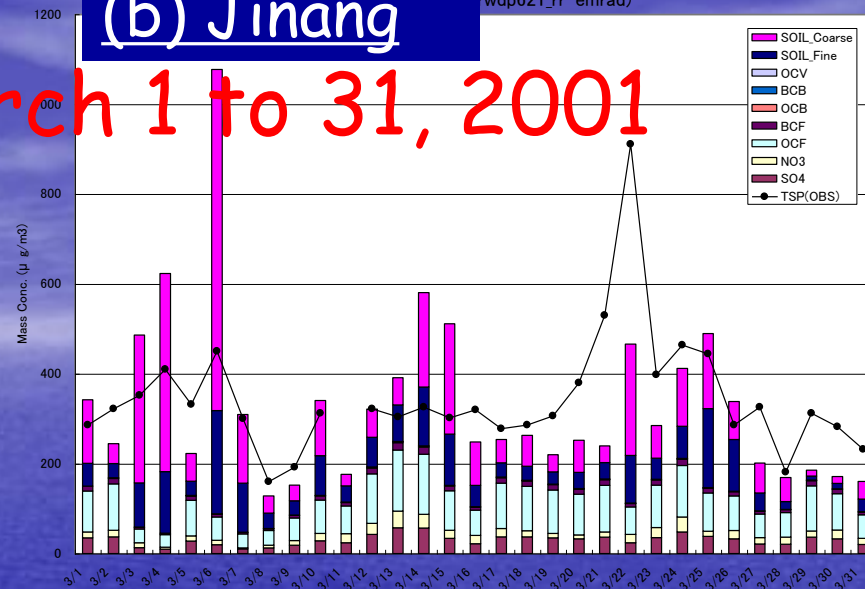
(a) Beijing

(rwdp721_rr-emrad)



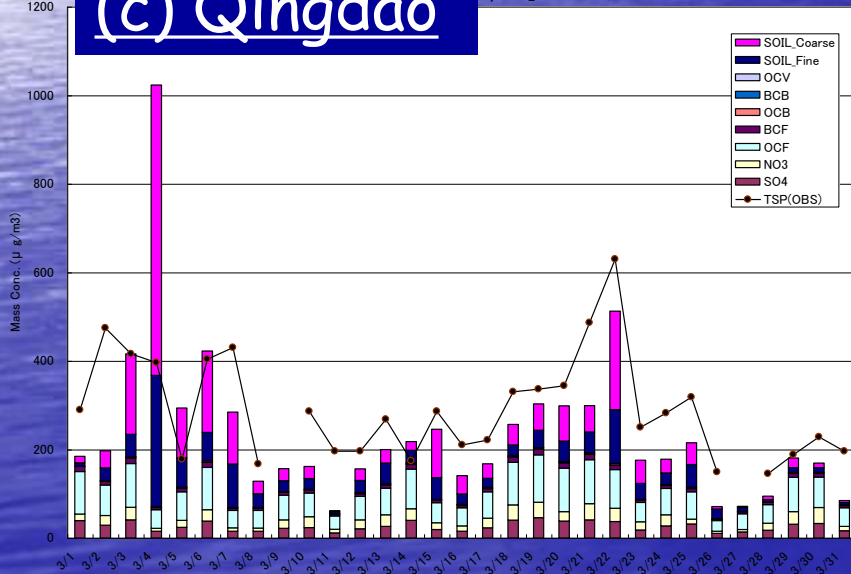
(b) Jinang

(rwdp621_rr-emrad)



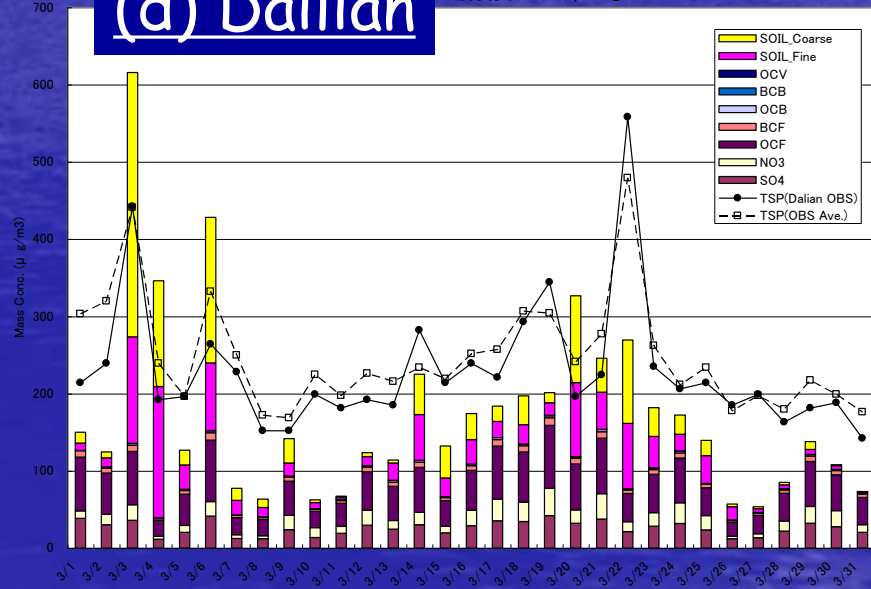
(c) Qingdao

(dp621_rr-emrad)



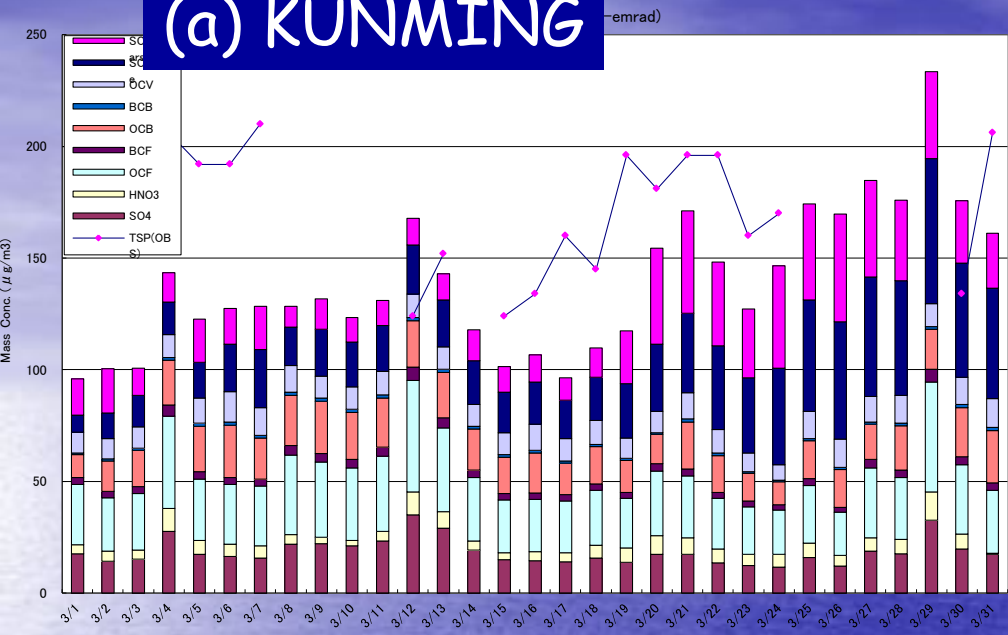
(d) Dailian

PM濃度変化 (rwdp821_rr-emrad)



Beijing & South or East of Beijing: 北京、齊南、青島、大連

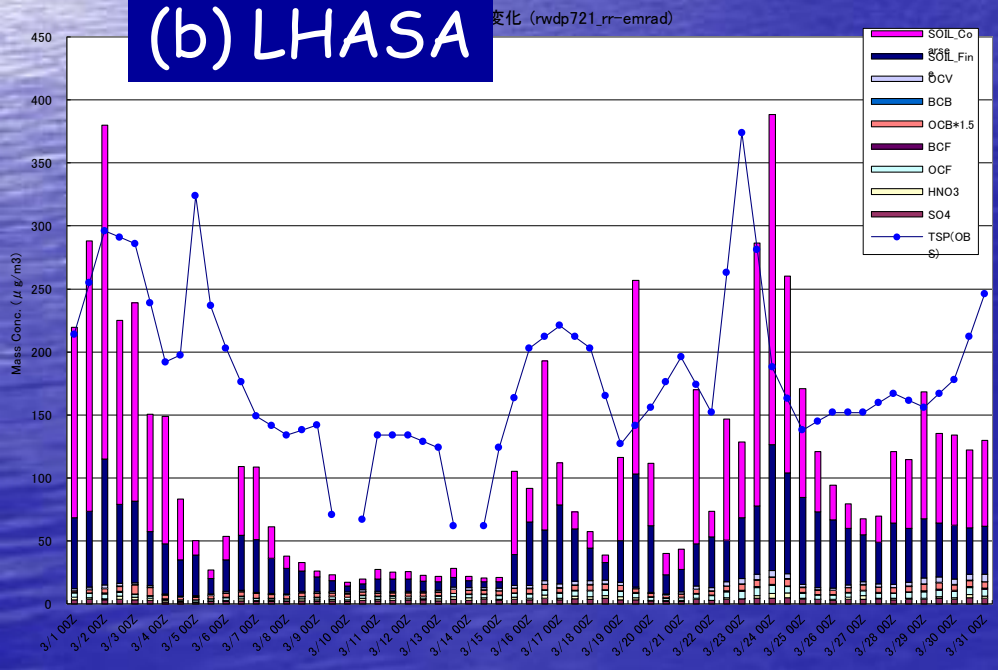
(a) KUNMING



Southeastern Mountainous Area:
Kunming(昆明)

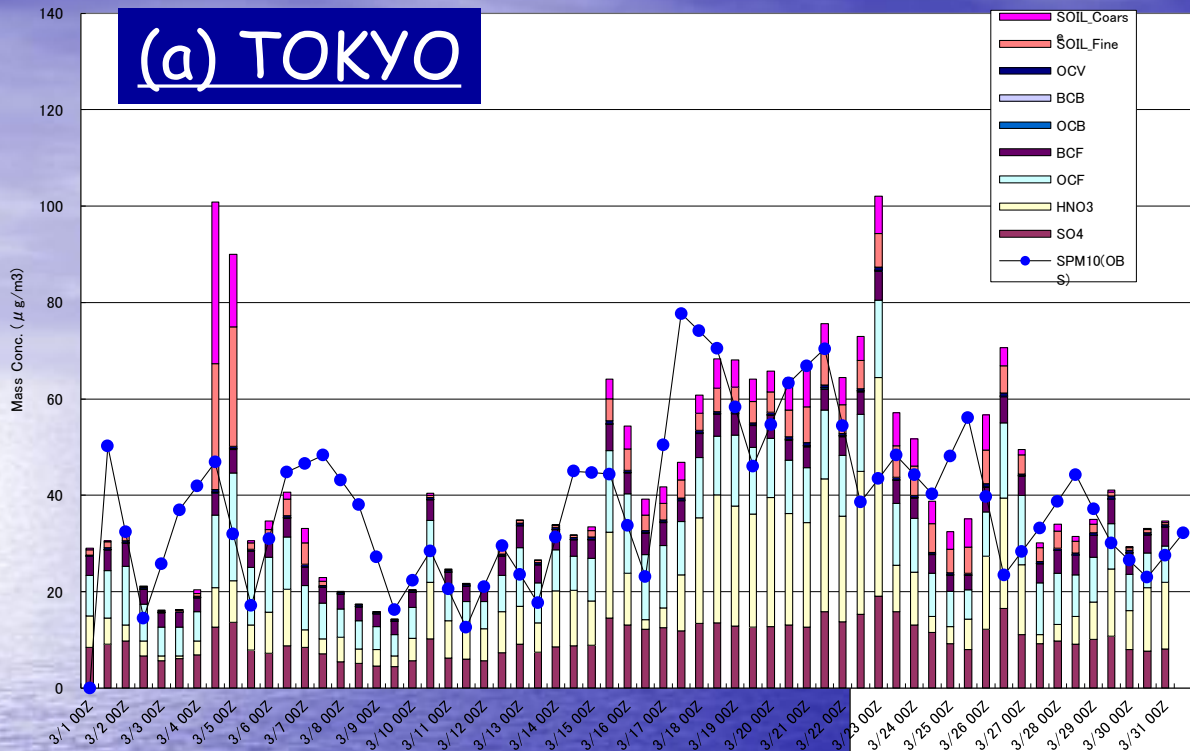
PM: Cal. Vs Obs. for March 1 to 31, 2001

(b) LHASA



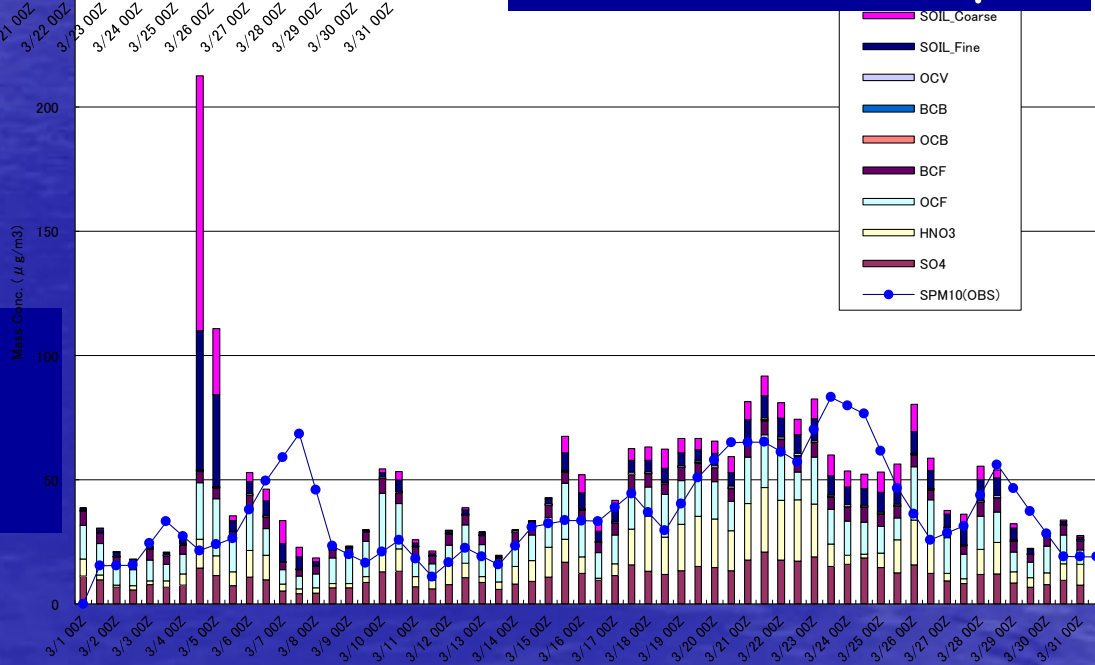
Southern Highland Area (Tibet): Lhasa(拉萨)

(a) TOKYO



SPM: Cal. Vs Obs. for March 1 to 31, 2001

(b) OSAKA, Japan



Japan: 東京、大阪

Summary and concluding remarks

- Introduced two examples of wet deposition modeling;
- (1) Cloud-resolving
- (2) Non Cloud-resolving simplified approach
- (3) Further investigation of the cloud-resolving study may be necessary for improvement of wet deposition prediction; the research will also improve parameterization in the non cloud-resolving approach.
- (4) Difficulty for mass balance study in the Fukushima case: Almost no information on atmospheric concentration fields of the discharged radioactive materials(?). Only deposition distribution is available. → Reduce other uncertainties such as met fields as much as possible.

One of the important factors: reliable Wet Deposition calculation.

- Three types of modeling;
 - (1) Dynamic Modeling using Three/Two Dimensional Cloud Transport Model: Cloud-Resolving Method → Allow trans-horizontal-grids mass transport of hydrometeors and chemical species with PDEs (Ex. Hegg et al. 1986, Rutledge et al. 1986, Kitada et al. 1993, others)
 - (2) Dynamic Modeling using One Dimensional Cloud Transport Model: Semi-Cloud-Resolving Method → Hydrometeors themselves are not transported over horizontal grid cells. (Ex. RSM - RADOM scavenging module, Berkowitz et al. 1989; PLUVIUS, Hales 1981, others); completes cloud processes within each vertical column.

One of the important factors: reliable
Wet Deposition calculation. (continued)

(3) Simple Modeling using Scavenging
Coefficient.